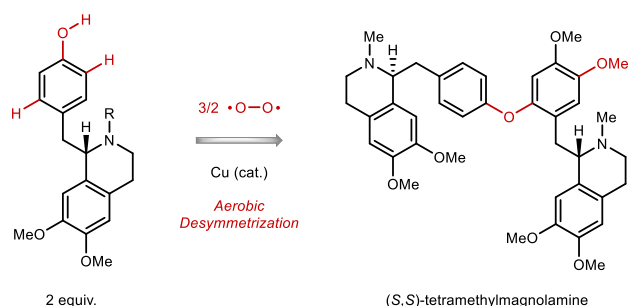


Total Synthesis of (*S,S*)-Tetramethylmagnolamine via Aerobic Desymmetrization

Zheng Huang, Xiang Ji,[†] and Jean-Philip Lumb^{*}

Department of Chemistry, McGill University, 801 Sherbrooke Street West, QC H3A 0B8, Canada

Supporting Information Placeholder

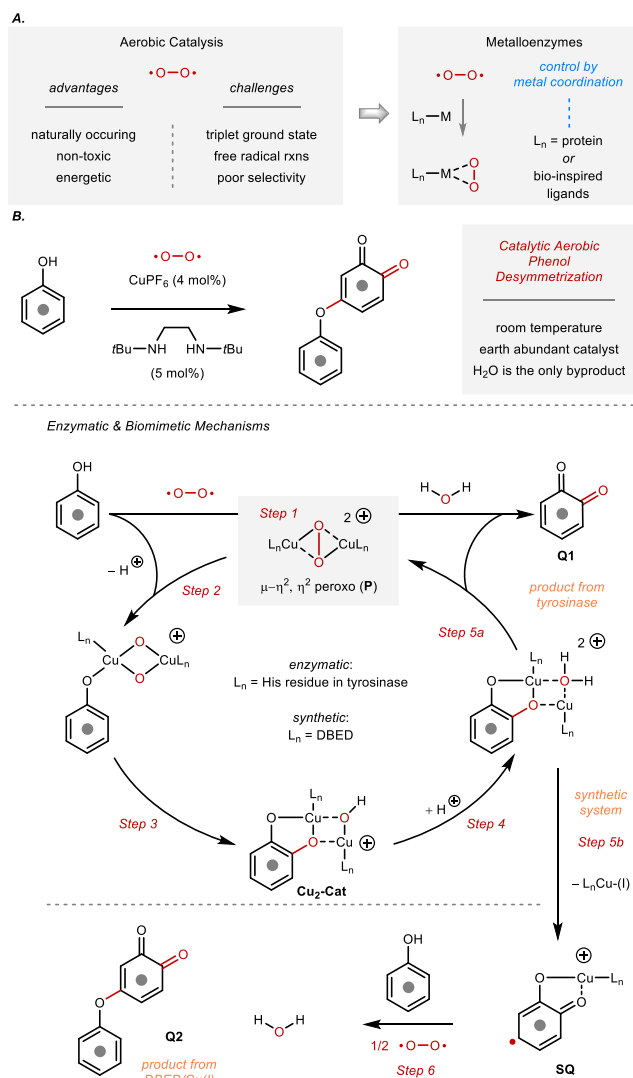


ABSTRACT: We describe a concise synthesis of the pseudo dimeric tetrahydroisoquinoline alkaloid (*S,S*)-tetramethylmagnolamine by a catalytic aerobic desymmetrization of phenols. Desymmetrization reactions increase molecular complexity with high levels of efficiency, but those that do so by aerobic oxidation are uncommon. Our conditions employ molecular oxygen as an oxygen atom transfer agent and a formal acceptor of hydrogen, enabling two, mechanistically distinct aromatic C-H oxygenation reactions with high degrees of selectivity.

Molecular oxygen (O_2) is an attractive reagent for chemical synthesis (Figure 1A).¹ It is renewable and non-toxic, and its reduction to water (H_2O) provides a strong thermodynamic driving force that can offset otherwise challenging bond forming reactions. Despite these advantages, O_2 can be difficult to use when oxidizing C-H bonds in complex molecules, where issues of chemo and regioselectivity outweigh synthetic efficiency.² O_2 has a small steric profile, a non-canonical $4 e^- | 4 \text{H}^+$ redox stoichiometry and a triplet electronic structure.³ These factors often lead to radical chain processes that can be difficult to control when potential sites of oxidation are not electronically differentiated.⁴

To overcome these challenges, our group has adopted a bio-inspired strategy of utilizing O_2 that is inspired by metalloenzymes (Scheme 1A).^{5,6} By coordinating O_2 to transition metals within their active sites, metalloenzymes can exert control over aerobic oxidations by defining the coordination environment surrounding the metal center.^{1a,1b,7} Our group has been particularly interested in the type III Cu-enzyme tyrosinase (Scheme 1B), which catalyzes the aerobic oxygenation of L-tyrosine in the first and rate limiting step of melanogenesis (not shown).⁸ Building upon bioinorganic studies of Stack and others,^{9,10} our group showed that the enzyme's mechanism of O_2 activation and oxygen atom transfer (OAT) could be recreated

by a simple and commercially available catalytic system, composed of $\text{Cu}(\text{CH}_3\text{CN})_4(\text{PF}_6)$ (abbreviated CuPF_6) and *N,N'*-di-*tert*-butylethylene diamine (DBED).¹¹ When applied to the oxidation of simple *para*-substituted phenols, this system catalyzes *ortho*-C-H oxygenation through a series of discrete steps consisting of: (*Step 1*) activation of O_2 as its di-Cu-(II) μ - η^2 , η^2 peroxy complex (**P**), (*Step 2*) coordination of a phenolate and (*Step 3*) electrophilic aromatic substitution onto the Cu_2O_2 core. While these discrete steps replicate those of the enzyme, the fate of the ensuing bridged di-Cu-(II)-catecholate (**Cu₂-Cat**) differs between the two systems. Whereas tyrosinase releases a free *ortho*-quinone (**Q1**) following (*Step 4*) protonation of the hydroxide bridge and (*Step 5a*) redox between the ligand and the metal centers, the synthetic system releases a Cu-(II)-semi-quinone radical complex (**SQ**) (*Step 5b*). The ensuing oxidative C-O coupling with the starting phenol is rate determining (*Step 6*), and provides the corresponding substituted *ortho*-quinone product (**Q2**) while releasing DBED-Cu-(I) to close the catalytic cycle.¹² O_2 serves multiple roles over the course of this reaction. The first is as a reagent for OAT that reduces the C_{2v} symmetry of the phenol to the C_s symmetry of either quinone (enzymatic) or **SQ** (biomimetic system). This distinction is important, since the retention of Cu in the **SQ** forces the biomimetic system to engage another equivalent of the starting phenol in a C-O coupling. This step is distinct from the first OAT,



Scheme 1. A) Bio-inspired strategies for the utilization of O₂. B) Biomimetic aerobic oxidation of phenol.

and ensures that the starting material is consumed in two distinct processes over the course of the reaction. C-O bond formation is driven by the favorable reduction of 1/2 O₂, highlighting its second role as a formal acceptor of H₂.

Herein, we wish to describe the application of this catalytic aerobic process to the synthesis of the pseudo-symmetric tetrahydroisoquinoline (**THIQ**) alkaloid (*S,S*)-tetramethylmagnolamine (**1**) (Scheme 2A). **1** is a member of the diaryl ether sub-family of **THIQs**, which encompass a number of structurally unique and biologically active members.¹³ Amongst them are the well-known macrocyclic diaryl ether tubocurarine (**4**),¹⁴ which is a potent muscle relaxant, and the chemotherapeutic (*S,S*)-thalicarpine (**3**).¹⁵ The family members share defining diaryl ethers, typically linking two, electron rich aromatic rings. They also possess two, basic amine functionalities separated by ~14 Å, which are believed to be protonated at physiological pH. This has become a defining structural feature of many simple, neuromuscular relaxants, which contain

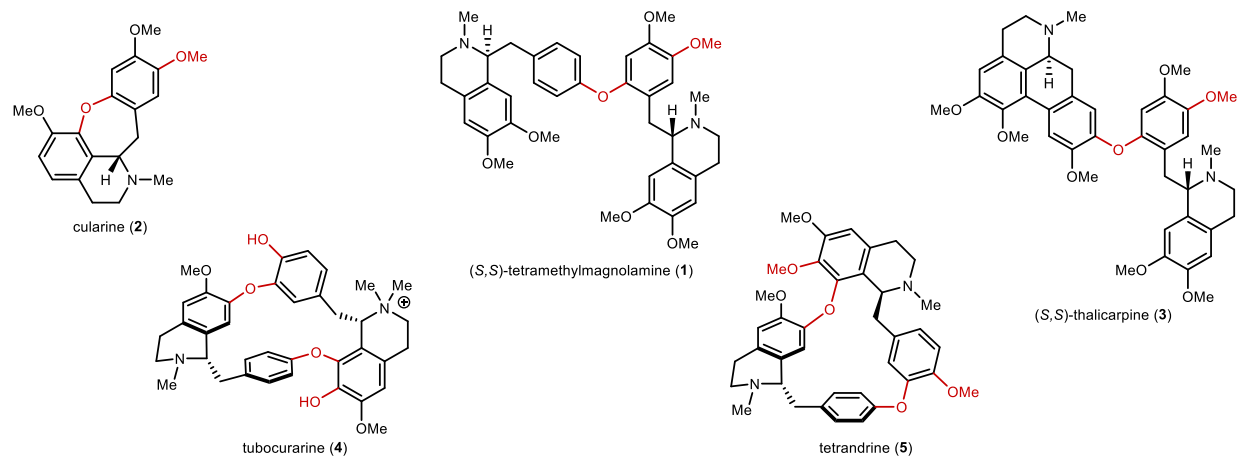
quaternized ammonium cations separated by ~10 carbon atoms.¹⁶

While this sub-family of **THIQs** has been extensively studied, questions remain about their biosynthesis, and how the associated oxidases create the defining diaryl ethers (Scheme 2B).^{13a} Free radical reactions of phenoxy radicals favor C-C instead of C-O bond formation, reflecting the favorable localization of spin density on the less electronegative carbons of the aromatic ring.^{1c,17} Little is known about how these enzymes change selectivity to promote C-O bond formation, and to what extent the metal center is involved in the bond forming event. This underscores a more general challenge of using phenols in oxidative C-O bond forming reactions, since it is easy to trigger competitive free-radical pathways that erode selectivity. Instead, more commonly practiced aryl ether syntheses are isohypsic, including Ullman or Buchwald-Hartwig cross coupling reactions that employ an oxidized aromatic halide as the coupling partner (Scheme 2C).¹⁸ Cross-coupling reactions of this family have been extensively studied, but their persistent use of stoichiometric base and elevated reaction temperatures makes them capricious in complex molecule settings. This includes the formation of the diaryl ether in (*S,S*)-tetramethylmagnolamine (**1**),¹⁹ which was synthesized by Opatz in 50% yield from phenol **9** and aryl bromide **10** under Ma's optimized conditions²⁰ for catalytic Ullman-type coupling.

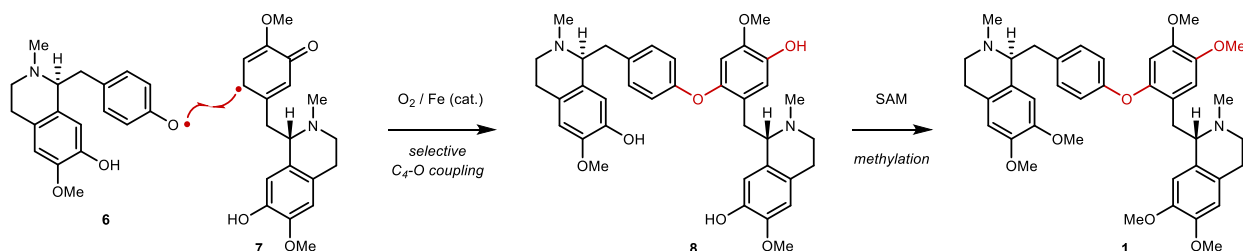
Recognizing that **1** possesses an element of hidden symmetry, we questioned whether our conditions for diaryl-ether formation could be used for its direct synthesis from **11** (Scheme 2C). This would feature a catalytic aerobic desymmetrization that could shorten the overall step count by requiring the preparation of only a single coupling partner. It would also offer a rare example of aerobic desymmetrization, in which an atom of O₂ is incorporated into the product.²¹ Herein, we describe the successful execution of this plan, and report a concise and high yielding synthesis of **1** along these lines.

To investigate our proposed key step, we developed an asymmetric synthesis of Boc-protected **THIQ** (**17**), inspired by the precedent of Noyori (Scheme 3).²² Namely, amidation of **12** and **13** at elevated temperatures without solvent, followed by a Bischler-Napieralski cyclization set the stage for Noyori's asymmetric hydrogenation.²² This introduced the benzylic stereocenter in 94% *e.e.* over a 3-step sequence that could be run on multi-gram scale in 70% yield. Despite our efforts to use free amine **16** or its methyl-substituted derivative (not shown) in the subsequent aerobic catalysis, these substrates afforded intractable mixtures at complete consumption of the starting material. Therefore, we advanced the synthesis by Boc-protection to afford **17** before conducting the key step. Under our previously optimized conditions,^{6a} aerobic oxidative coupling is complete within 4 h at room temperature using an applied pressure of O₂ (1 atm). The catalyst system is composed of 4 mol% CuPF₆ and 5 mol% of DBED in CH₂Cl₂. While *ortho*-quinone **19** is the immediate product of coupling, we use a reductive work-up, consisting of a saturated aqueous solution of sodium dithionite (Na₂S₂O₄), to effect *in situ* reduction. This leads to the corresponding coupled catechol **20** in a 60% isolated yield on 400 mg

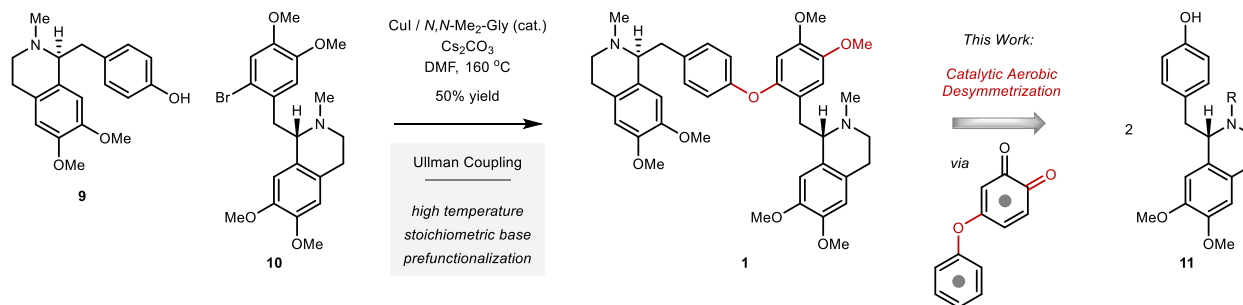
A. Isoquinoline Diaryl Ethers



B. Proposed Biosynthesis



C. Previous Synthesis & This Work

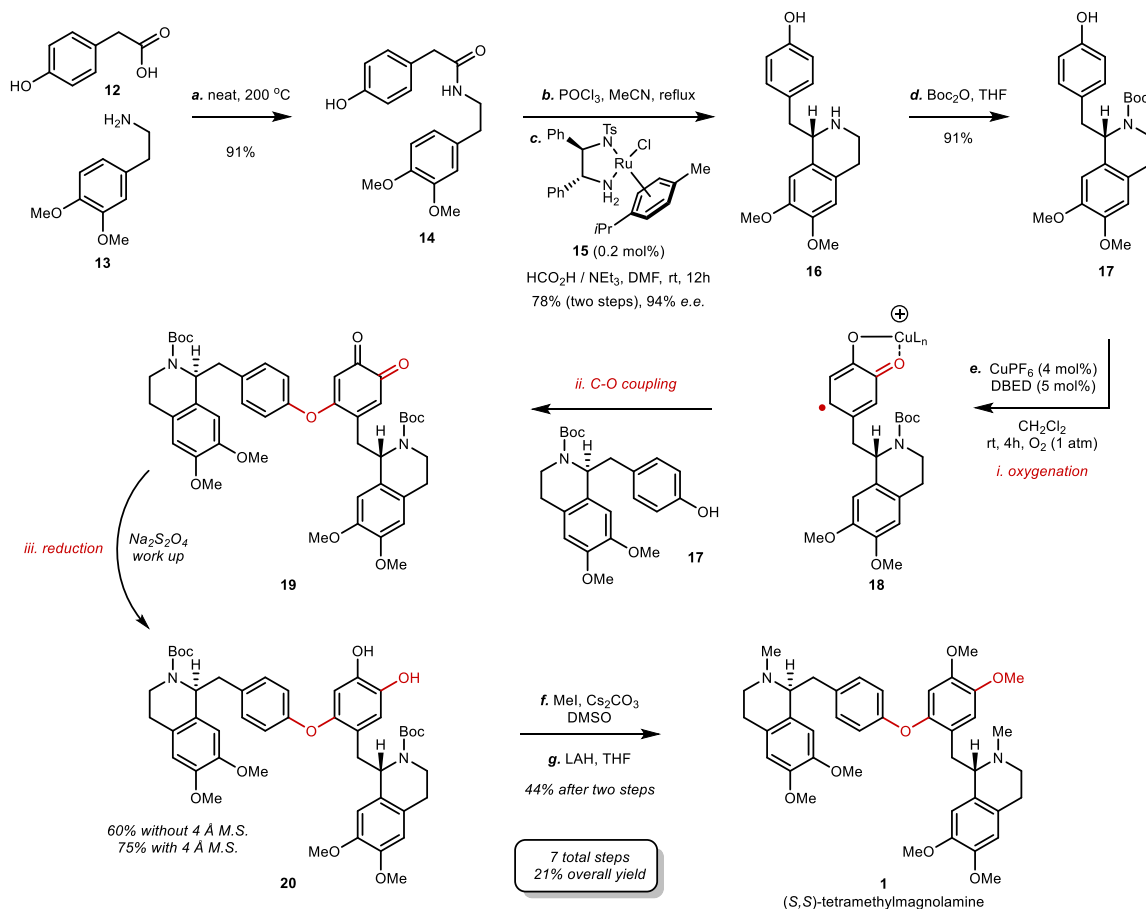


Scheme 2. A) Tetrahydroisoquinoline alkaloids with diarylether linkages. B) Proposed biosynthesis of the diarylether linkages. C) Previous synthesis of (*S,S*)-tetramethylmagnolamine and this work.

scale. Notably, the yield of this process improves to 75% when conducted in the presence of 4Å M.S., highlighting the beneficial effects of running these reactions in the presence of a desiccant.^{17b} Subsequent methylation of the catechol and reduction of the *N*-Boc groups under standard conditions furnished (*S,S*)-tetramethylmagnolamine (**1**) in a longest linear sequence (LLS) of 7 steps that proceeded in 21% overall yield. This compares favorably to the only previous synthesis of **1** by Opatz (Scheme 2C), which required 16 total steps and a LLS of 8 steps that proceeded in 14% overall yield.¹⁹ Our route takes advantage of the target's pseudo symmetry, and forms the key aryl ether linkage at room temperature by selectively oxidizing two aromatic C-H bonds of one equivalent of the starting material and the phenol O-H on another. Because O_2 is the terminal reductant, H_2O is the only stoichiometric byproduct of the reaction.

In conclusion, we have described an asymmetric total synthesis of (*S,S*)-tetramethylmagnolamine (**1**) that fea-

tures a catalytic aerobic desymmetrization of phenols. Despite many of its attributes, O_2 remains underutilized in complex molecule synthesis, due, in part, to persistent challenges of controlling selectivity. Our work highlights the beneficial effects of bioinspired metal-coordination in overcoming this challenge, and also highlights the unique reactivity of Cu in catalyzing C-O bond formation during phenolic oxidation. We see many opportunities to extend this chemistry to other diaryl ether targets, including additional members of the **THIQ**-ether sub-family, and work towards this goal will be reported in due course.



Scheme 3. Forward Synthesis. Reagents and conditions: a) neat, 200 °C, 2 h, 91%; b) POCl₃ (6 equiv.), MeCN, reflux, 1 h; c) **15** (0.2 mol%), HCO₂H/NEt₃ (5:2), DMF, rt, 12 h, 78% over 2 steps, 94% e.e.; d) Boc₂O (1.1 equiv.), MeOH, rt, 12 h, 89%; e) [Cu(MeCN)₄](PF₆) (4 mol%), DBED (5 mol%), 4 Å M.S., CH₂Cl₂, O₂ (1 atm), rt, 4 h, then Na₂S₂O₄ work up, 75%; f) MeI (3.0 equiv.), Cs₂CO₃ (3.0 equiv.), DMSO, rt, 12 h; g) LiAlH₄ (10.0 equiv.), THF, reflux, 12 h, 44% over 2 steps.

ASSOCIATED CONTENT

Supporting Information

The Supporting Information is available free of charge on the ACS Publications website.

Experimental procedures, characterization data, copies of NMR spectra (PDF)

AUTHOR INFORMATION

Corresponding Author

* jean-philip.lumb@mcgill.ca

Present Addresses

†Department of Chemistry, New York University, Silver Center for Arts and Science, 100 Washington Square East, New York, NY 10003, United States

Notes

The authors declare no competing financial interest.

ACKNOWLEDGMENT

Financial support was provided by the Natural Sciences and Engineering Council (NSERC) of Canada (Discovery Grant to J.-P. L.); the Fonds de Recherche Quebecois Nature et

Technologies (FRQNT) (Team Grant to J.-P. L.); McGill University Faculty of Science (Milton Leong Fellowship in Science to Z. H.) the FRQNT Center for Green Chemistry and Catalysis (Fellowship to X. J.).

REFERENCES

- (a) Que, L.; Tolman, W. B. *Nature* **2008**, *455*, 333-340; (b) Trammell, R.; Rajabimoghadam, K.; Garcia-Bosch, I. *Chem. Rev.* **2019**; (c) Allen, S. E.; Walvoord, R. R.; Padilla-Salinas, R.; Kozlowski, M. C. *Chem. Rev.* **2013**, *113*, 6234-6458; (d) Campbell, A. N.; Stahl, S. S. *Acc. Chem. Res.* **2012**, *45*, 851-863; (e) Punniyamurthy, T.; Velusamy, S.; Iqbal, J. *Chem. Rev.* **2005**, *105*, 2329-2364.
- Stahl, S. S.; Alsters, P. L., *Liquid Phase Aerobic Oxidation Catalysis: Industrial Applications and Academic Perspectives*. Wiley-VCH: Weinheim, 2016.
- Borden, W. T.; Hoffmann, R.; Stuyver, T.; Chen, B. J. *Am. Chem. Soc.* **2017**, *139*, 9010-9018.
- (a) Esguerra, K. V. N.; Xu, W.; Lumb, J.-P. *Chem* **2017**, *2*, 533-549; (b) Esguerra, K. V. N.; Lumb, J.-P. *Angew. Chem. Int. Ed.* **2018**, *57*, 1514-1518.
- For review articles, see: (a) Esguerra, K. V. N.; Lumb, J.-P. *Synthesis* **2019**, *51*, 334-358; (b) Huang, Z.; Lumb, J.-P. *ACS Catal.* **2019**, *9*, 521-555.
- For related examples, see: (a) Esguerra, K. V. N.; Fall, Y.; Lumb, J.-P. *Angew. Chem.* **2014**, *126*, 5987-5991; (b) Huang, Z.;

- Kwon, O.; Huang, H.; Fadli, A.; Marat, X.; Moreau, M.; Lumb, J.-P. *Angew. Chem. Int. Ed.* **2018**, *57*, 11963-11967.
7. (a) Elwell, C. E.; Gagnon, N. L.; Neisen, B. D.; Dhar, D.; Spaeth, A. D.; Yee, G. M.; Tolman, W. B. *Chem. Rev.* **2017**, *117*, 2059-2107; (b) Solomon, E. I.; Heppner, D. E.; Johnston, E. M.; Ginsbach, J. W.; Cirera, J.; Qayyum, M.; Kieber-Emmons, M. T.; Kjaergaard, C. H.; Hadt, R. G.; Tian, L. *Chem. Rev.* **2014**, *114*, 3659-3853.
8. (a) Borovansky, J.; Riley, P. A., *Melanins and Melanosomes*. Wiley-VCH: Weinheim, 2011; (b) Esguerra, K. V. N.; Lumb, J.-P. *Synlett* **2015**, *26*, 2731-2738.
9. Mirica, L. M.; Vance, M.; Rudd, D. J.; Hedman, B.; Hodgson, K. O.; Solomon, E. I.; Stack, T. D. P. *Science* **2005**, *308*, 1890-1892.
10. For review articles, see: (a) Rolff, M.; Schottenheim, J.; Decker, H.; Tuczek, F. *Chem. Soc. Rev.* **2011**, *40*, 4077-4098; (b) Mirica, L. M.; Ottenwaelder, X.; Stack, T. D. P. *Chem. Rev.* **2004**, *104*, 1013-1046.
11. Askari, M. S.; Esguerra, K. V. N.; Lumb, J.-P.; Ottenwaelder, X. *Inorg. Chem.* **2015**, *54*, 8665-8672.
12. For a more detailed study of the C-O coupling step, see: Huang, Z.; Lumb, J.-P. *Angew. Chem. Int. Ed.* **2016**, *55*, 11543-11547.
13. (a) "Chapter One - Bisbenzylisoquinoline Alkaloids": Weber, C.; Opatz, T. In *The Alkaloids: Chemistry and Biology*, Knölker, H.-J., Ed. Academic Press: 2019; Vol. 81, pp 1-114; (b) Shamma, M., *The isoquinoline alkaloids chemistry and pharmacology*. Elsevier: 2012; Vol. 25.
14. Otto, N.; Ferenc, D.; Opatz, T. *J. Org. Chem.* **2017**, *82*, 1205-1217.
15. (a) Kupchan, S. M.; Liepa, A. J.; Kameswaran, V.; Sempuku, K. *J. Am. Chem. Soc.* **1973**, *95*, 2995-3000; (b) Xu, W.; Huang, Z.; Ji, X.; Lumb, J.-P. *ACS Catal.* **2019**, *9*, 3800-3810.
16. "Alkaloids": Dewick, P. M. In *Medicinal Natural Products*, Dewick, P. M., Ed. 2009; pp 311-420.
17. (a) "3.13 Oxidative Coupling of Phenols and Phenol Ethers": Quideau, S.; Deffieux, D.; Pouységu, L. In *Comprehensive Organic Synthesis II (Second Edition)*, Knochel, P., Ed. Elsevier: Amsterdam, 2014; pp 656-740; (b) Esguerra, K. V. N.; Fall, Y.; Petitjean, L.; Lumb, J.-P. *J. Am. Chem. Soc.* **2014**, *136*, 7662-7668.
18. (a) Evano, G.; Wang, J.; Nitelet, A. *Organic Chemistry Frontiers* **2017**, *4*, 2480-2499; (b) Pitsinos, E. N.; Vidali, V. P.; Couladouros, E. A. *Eur. J. Org. Chem.* **2011**, *2011*, 1207-1222.
19. Blank, N.; Opatz, T. *J. Org. Chem.* **2011**, *76*, 9777-9784.
20. Ma, D.; Cai, Q. *Org. Lett.* **2003**, *5*, 3799-3802.
21. For selected examples of desymmetrization in biosynthesis or bioinspired synthesis, see: Hu, X.; Maimone, T. J. *J. Am. Chem. Soc.* **2014**, *136*, 5287-5290; ; (b) Miyabe, H.; Torieda, M.; Inoue, K.; Tajiri, K.; Kiguchi, T.; Naito, T. *J. Org. Chem.* **1998**, *63*, 4397-4407; (c) Smith, W. L.; Urade, Y.; Jakobsson, P.-J. *Chem. Rev.* **2011**, *111*, 5821-5865; (d) Goodhue, C. T.; Schaeffer, J. R. *Biotechnol. Bioeng.* **1971**, *13*, 203-214.
22. Uematsu, N.; Fujii, A.; Hashiguchi, S.; Ikariya, T.; Noyori, R. *J. Am. Chem. Soc.* **1996**, *118*, 4916-4917.
-

Total Synthesis of (*S,S*)-Tetramethylmagnolamine via Aerobic Desymmetrization

Zheng Huang, Xiang Ji, Jean-Philip Lumb*

Department of Chemistry, McGill University, Montreal, QC, H3A 0B8, Canada

Table of Contents

1. General Experimental.....	2
2. Synthesis and Characterization of Compounds in Scheme 3.....	3
3. NMR Comparison of (<i>S,S</i>)-Tetramethylmagnolamine.....	9
4. References and Notes.....	10
5. Copies of ¹ H and ¹³ C NMR spectra.....	11

1. General Experimental

Purchasing and purification of reagents:

Chemicals and solvents were purchased from Sigma Aldrich, Alfa Aesar, Strem Chemicals, TCI or Oakwood, and used as received without further purification. $[\text{Cu}(\text{MeCN})_4](\text{PF}_6)$ (97%) was purchased from Sigma Aldrich, and stored under an inert atmosphere. Solvents were dried and purified using a PureSolv MD 7 (from Innovative Technology) or MB SPS 800 (from MBraun). We have not observed differences in the reaction outcome using either of these solvent purifiers. Unless otherwise noted, solvent was degassed by sparging N_2 for 10 min at rt prior to use. Molecular sieves (4 Å, powdered and “activated”) were purchased from Sigma Aldrich and were flame-dried with a torch in the reaction vessel immediately prior to use.

Acquisition and analysis of NMR data:

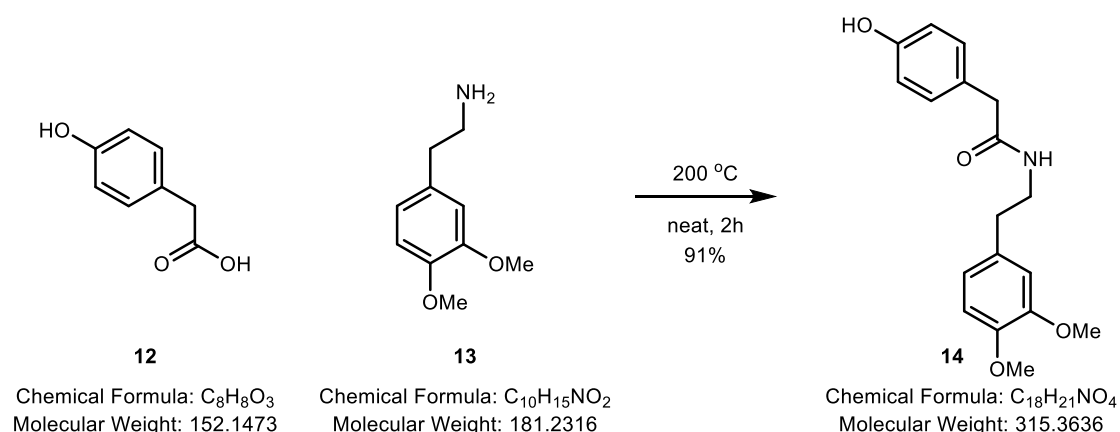
Proton nuclear magnetic resonance (^1H NMR) spectra were acquired using Bruker Ascend 500 MHz or 400 MHz spectrometers. Chemical shifts (δ) are reported in parts per million (ppm) and are calibrated to the residual solvent peak. Coupling constants (J) are reported in Hz. Multiplicities are reported using the following abbreviations: s = singlet; d = doublet; t = triplet; q = quartet; br = broad; m = multiplet (range of multiplet is given). Carbon nuclear magnetic resonance (^{13}C NMR) spectra were acquired using Bruker Ascend 126 MHz or 101 MHz spectrometers. Chemical shifts (δ) are reported in parts per million (ppm) and are calibrated to the residual solvent peak.

Additional information:

High resolution mass spectra (HRMS) were recorded using a Bruker maXis Impact TOF mass spectrometer by electrospray ionization time of flight reflectron experiments. Fourier-transform infrared (FT-IR) spectra were recorded on a Bruker Alpha FT-IR spectrometer. Optical rotations were recorded on a Perkin–Elmer 341 polarimeter (using the sodium D line; 589 nm). High performance liquid chromatography (HPLC) was measured on an Agilent 1200 Infinity Series HPLC system. Analytical thin-layer chromatography was performed on pre-coated 250 mm layer thickness silica gel 60 F254 plates (EMD Chemicals Inc). Visualization was performed by ultraviolet light and/or by staining with potassium permanganate or cerium molybdate. Purifications by column chromatography were performed using standard column chromatography using silica gel (40-63 μm , 230-400 mesh). All reactions that utilize molecular oxygen (O_2) were performed with an applied pressure at 1.0 atm in Radley tubes.

2. Synthesis and Characterization of compounds in Scheme 3

Compound 14

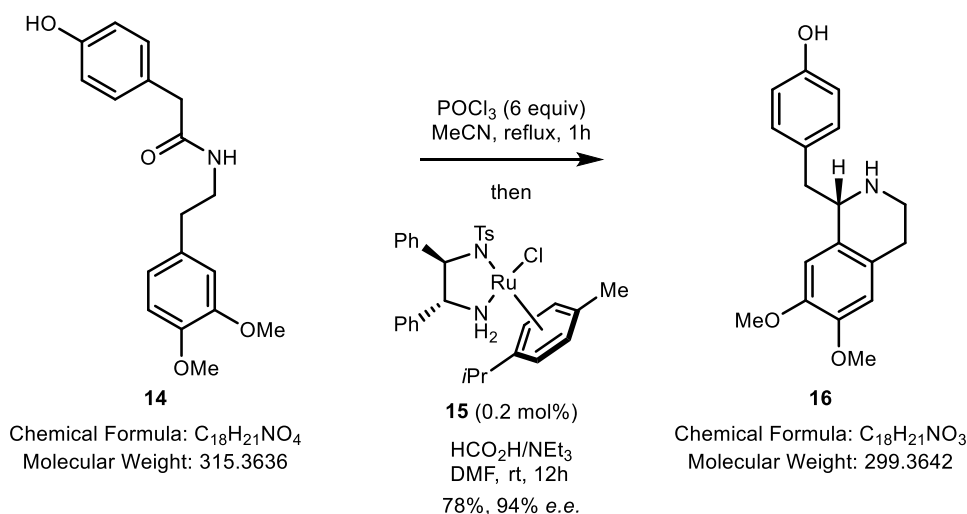


Procedure: A 100 mL flame-dried high-pressure tube equipped with a Teflon-coated stir bar and a threaded screw cap was charged with 4-hydroxyphenylacetic acid (**12**) (50 mmol, 7.61 g, 1.0 equiv) and 3, 4-dimethoxyphenethylamine (**13**) (50 mmol, 8.44 mL, 1.0 equiv). The mixture was purged with N_2 for 5 min, prior to sealing the reaction vessel and heating to 200 °C in a pre-heated oil bath for 2h. The reaction mixture was then cooled to room temperature, the mixture was dilute with CH_2Cl_2 (100 mL), and poured onto HCl (1 M, 100 mL), and washed with CH_2Cl_2 (3×100 mL). The combined organic layers were washed with saturated $NaHCO_3$ (100 mL), brine (50 mL) and dried over $MgSO_4$. The organic layer was filtered and concentrated *in vacuo* to provide **14** (14.4 g, 45.5 mmol, 91%) as a tan solid, which was used for the next step without further purification.

Characterization:

1H NMR (500 MHz, $CDCl_3$) δ 6.99 (d, $J = 8.5$ Hz, 2H), 6.76 (d, $J = 8.5$ Hz, 2H), 6.74 (d, $J = 8.2$ Hz, 1H), 6.60 (d, $J = 1.9$ Hz, 1H), 6.55 (dd, $J = 8.1, 2.0$ Hz, 1H), 5.41 (br s, 1H), 3.86 (s, 3H), 3.82 (s, 3H), 3.49 – 3.40 (m, 4H), 2.68 (t, $J = 6.9$ Hz, 2H); ^{13}C NMR (126 MHz, $CDCl_3$) δ 171.9, 155.5, 149.2, 147.8, 131.2, 130.8, 126.4, 120.8, 116.1, 112.0, 111.6, 56.1, 56.0, 43.0, 40.9, 35.1. Our characterization data matches literature reports.¹

Compound 16

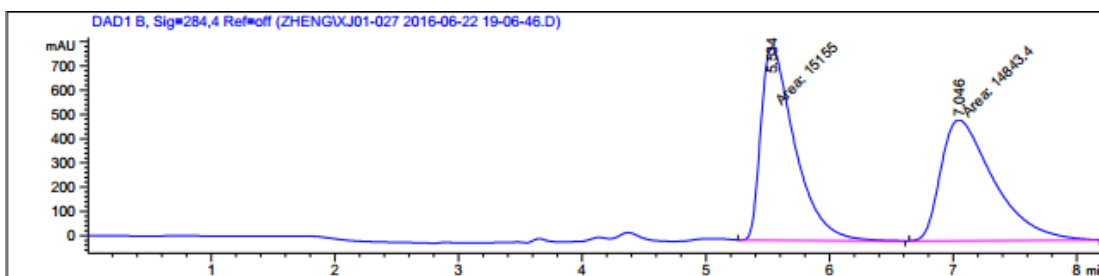


Procedure: A 500 mL flame-dried round-bottom flask equipped with a Teflon-coated stir bar was charged **14** (30 mmol, 9.46 g, 1.0 equiv) and dry and degassed MeCN (150 mL). $POCl_3$ (180 mmol, 16.83 mL, 6.0 equiv) was then slowly added to the mixture via syringe, and the resulting reaction mixture was refluxed for 1h. The reaction mixture was then cooled to room temperature, and all volatile compounds were removed at reduced pressure. Water (150 mL) was then added, and the resulting mixture was refluxed for another 2h. The flask was then cooled to 0 °C in an ice bath, and an aqueous solution of NaOH (2M, 150 mL) was added slowly to neutralize the reaction mixture. The reaction pH was further adjusted to pH 7-8 with saturated $NaHCO_3$ or 1 M HCl, at which point the intermediate imine precipitated as a yellow to brown solid. The solid was then separated by filtration, and the filtrate was washed with CH_2Cl_2 (3 × 100 mL). The combined organic layers were dried over Na_2SO_4 , filtered and concentrated *in vacuo*. The two sources of imine were then combined, and used for the reduction without further purification. A 250 mL flame-dried round-bottom flask equipped with a Teflon-coated stir bar and a rubber septa was charged with the crude imine and (*R,R*)-Ru(Ts-DPEN)(*p*-cymene)Cl (**15**, 38.2 mg, 0.06 mmol, 0.2 mol%). The reaction vessel was then evacuated and backfilled with N_2 (3 x) before adding a 5:2 molar mixture of HCO_2H and NEt_3 (7.5 mL) and dry and degassed DMF (30 mL) via syringe. The mixture was stirred at room temperature (ca. 23 °C) for 12h. The mixture was then poured onto saturated $NaHCO_3$ (150 mL) and washed with CH_2Cl_2 (3 × 150 mL). The combined organic layers were then washed with water (200 mL), brine (100 mL) and dried over Na_2SO_4 . The organic layer was then filtered and concentrated *in vacuo*. The crude mixture was purified by column chromatography on silica gel (CH_2Cl_2 :MeOH 20:1 to 5% NEt_3 in CH_2Cl_2 :MeOH 5:1) to provide **16** (7.02 g, 23.4 mmol, 78%, 94% e.e.) as a green solid.

Characterization:

1H NMR (500 MHz, $CDCl_3$) δ 6.96 (d, J = 8.2 Hz, 2H), 6.62 (d, J = 8.1 Hz, 2H), 6.56 (s, 1H), 6.55 (s, 1H), 6.45 (br s, 2H), 4.15 (dd, J = 7.7, 5.0 Hz, 1H), 3.81 (s, 3H), 3.76 (s, 3H), 3.29 – 3.16 (m, 1H), 3.08 (dd, J = 13.6, 4.0 Hz, 1H), 3.01 – 2.85 (m, 2H), 2.82 – 2.68 (m, 2H); ^{13}C NMR (126 MHz, $CDCl_3$) δ 155.9, 147.6, 147.1, 130.3, 128.7, 128.3, 126.3, 116.0, 111.6, 109.6, 56.4, 55.9, 55.7, 41.1, 39.6, 28.3. HPLC (chiralcel OD-H analytical column, eluent 0.1% $HNEt_2$ in 4:6 $iPrOH$:hexanes, 1 mL/min) t_R 5.5 min (major), 7.0 min (minor), 94% e.e.. $[\alpha]^{25}_D$ -23°, (c = 1.0, $CHCl_3$), [lit. -24°, (c = 0.2, $CHCl_3$)]. Our characterization data matches literature reports.²

HPLC of the racemic mixture:

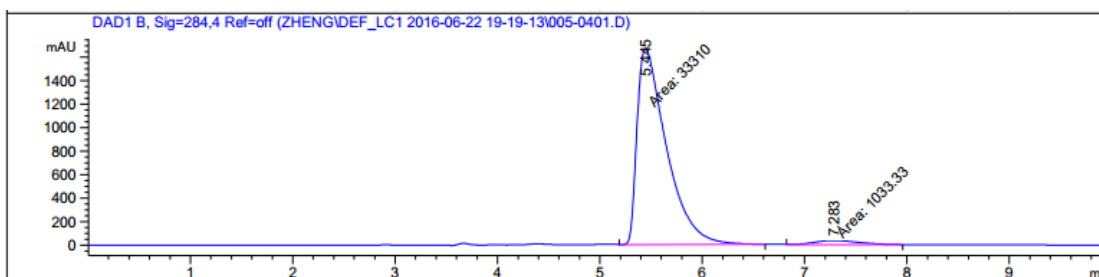


Peak #	RetTime [min]	Type	Width [min]	Area [mAU*s]	Height [mAU]	Area %
1	5.534	MM	0.3171	1.51550e4	796.60956	50.5194
2	7.046	MM	0.4966	1.48434e4	498.16376	49.4806

Totals : 2.99984e4 1294.77332

=====

HPLC of the chiral product (94% e.e.):

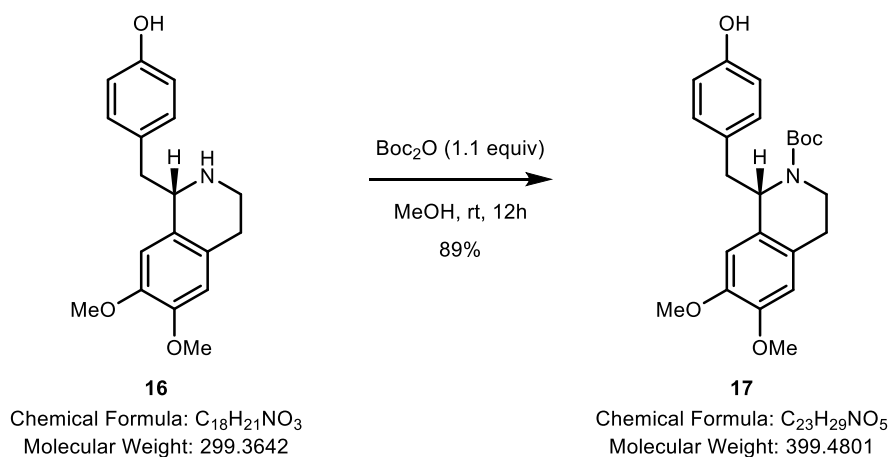


Peak #	RetTime [min]	Type	Width [min]	Area [mAU*s]	Height [mAU]	Area %
1	5.445	MM	0.3322	3.33100e4	1671.12305	96.9912
2	7.283	MM	0.4965	1033.33008	34.68862	3.0088

Totals : 3.43434e4 1705.81167

=====

Compound 17

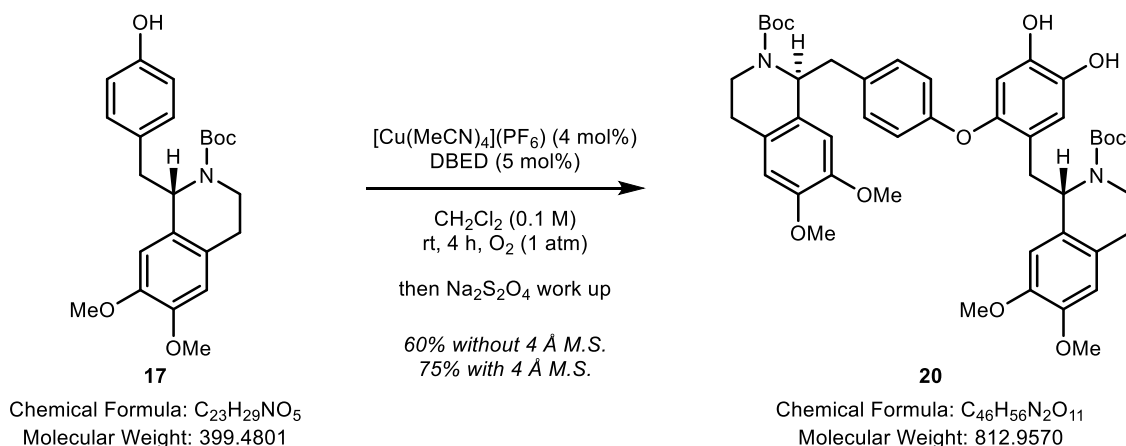


Procedure: A 100 mL flame-dried round-bottom flask equipped with a Teflon-coated stir bar was charged with **16** (10 mmol, 2.99 g, 1.0 equiv) and Boc₂O (11 mmol, 2.40 g, 1.1 equiv). The reaction vessel was evacuated and backfilled with N₂ (3 x), prior to the addition of dry and degassed MeOH (20 mL). The reaction mixture was then concentrated *in vacuo*, and the crude product was purified by column chromatography on silica gel (hexanes:EtOAc 2:1) to provide **17** (3.56 g, 8.9 mmol, 89%) as an off white solid.

Characterization:

¹H NMR (500 MHz, CDCl₃, mixture of rotamers) δ 7.02 and 6.95 (d, *J* = 8.2 Hz, 2H), 6.91 and 6.14 (br s, 1H), 6.79 and 6.70 (d, *J* = 8.3 Hz, 2H), 6.62 and 6.58 (s, 1H), 6.50 and 6.17 (s, 1H), 5.19 and 5.10 (t, *J* = 6.6 Hz, 1H), 4.26 and 3.86 (ddd, *J* = 12.8, 5.3, 3.0 Hz, 1H), 3.86 and 3.84 (s, 3H), 3.82 and 3.62 (s, 3H), 3.41 – 3.20 (m, 1H), 3.09 – 2.72 (m, 3H), 2.64 – 2.55 (m, 1H), 1.44 and 1.25 (s, 9H); **¹³C NMR** (126 MHz, CDCl₃, mixture of rotamers) δ 155.5, 154.8, 147.9, 147.6, 147.4, 146.9, 131.0, 130.8, 130.2, 129.8, 129.0, 128.8, 126.6, 126.3, 115.3, 115.2, 111.7, 111.3, 110.9, 110.4, 80.3, 79.9, 56.7, 56.1, 56.05, 55.99, 55.9, 55.8, 42.0, 39.4, 37.1, 28.6, 28.4, 28.3. [α]_D²⁵ +67°, (*c* = 1.0, CHCl₃). Our characterization data matches literature reports.³

Compound 20



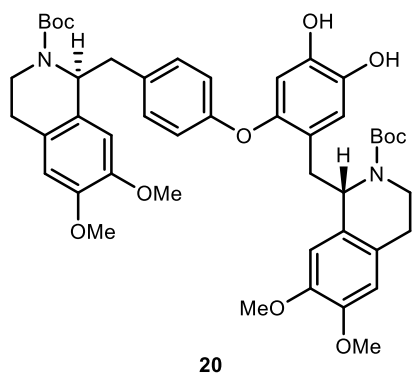
Procedure: A flame-dried, 25 mL Radley tube equipped with a Teflon-coated stir bar and a rubber septa was charged with $[Cu(CH_3CN)_4](PF_6)$ ($CuPF_6$, 29.8 mg, 0.08 mmol, 4 mol%) and **17** (0.5 mmol, 799.0 mg, 1.0 equiv). The reaction vessel was then evacuated and backfilled with N_2 (3 x), prior to the addition of *N,N'*-di-*tert*-butylethylenediamine (21.6 μ L, 0.025 mmol, 5 mol%) and dry and degassed CH_2Cl_2 (20 mL). The rubber septa was then rapidly removed and replaced with a Radley cap, which was connected to a tank of O_2 and pressurized to 1 atm. Under a constant pressure of O_2 (1 atm), the reaction vessel was vented 3 times for 10 s to remove N_2 . A dramatic color change was observed within 2 min, resulting in a blackish/brown reaction mixture. The reaction mixture was then stirred at room temperature (20–23 $^{\circ}C$) for 4h, depressurized by opening to the atmosphere and quenched by the addition of $Na_2S_2O_4$ (10 mL, saturated aqueous solution). The biphasic mixture was stirred vigorously for 1 min, during which time the dark red color of the organic phase changed to a yellow color. The phases were then separated, and the aqueous phase was washed with CH_2Cl_2 (3 \times 20 mL). The combined organic fractions were then dried over $MgSO_4$, filtered and concentrated *in vacuo*. The crude product was purified by column chromatography on silica gel (hexanes:EtOAc 1:2), to provide **20** (490.1 mg, 0.603 mmol, 60%) as a pale-yellow solid.

Modification: In a separate experiment, we observed beneficial effects of including 4 \AA mol. sieves (400 mg). These were added directly to the reaction vessel at the beginning of the reaction, and improved the isolated yield of **20** to 75%.

Characterization:

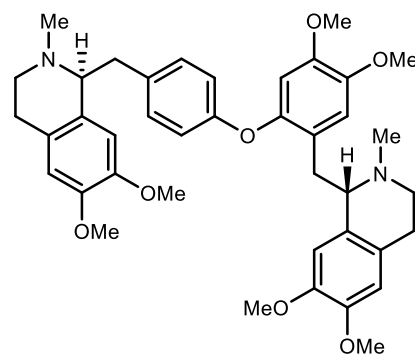
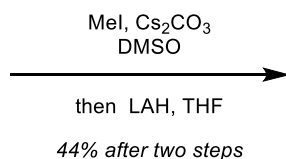
R_f = (EtOAc:Hexanes 2:1): 0.22; IR (neat) ν = 3288, 2931, 1682, 1658, 1515, 1503, 1420, 1364, 1221, 1158, 1123 cm^{-1} ; 1H NMR (500 MHz, $CDCl_3$, mixture of rotamers) δ 7.17 – 6.13 (m, 12H), 5.38 – 4.98 (m, 2H), 4.62 – 3.92 (m, 2H), 3.84, 3.83, 3.81, 3.80, 3.73, 3.71, 3.70, 3.65, 3.64, 3.62 (s, 12H), 3.42 – 3.17 (m, 2H), 3.15 – 2.53 (m, 8H), 1.40, 1.38, 1.30, 1.22, 1.12, 1.11 (s, 18H); ^{13}C NMR (126 MHz, $CDCl_3$, mixture of rotamers) δ 157.3, 157.0, 155.1, 154.9, 154.8, 154.7, 147.9, 147.8, 147.4, 147.3, 147.1, 146.9, 144.2, 144.0, 140.8, 140.6, 132.3, 132.0, 131.1, 130.9, 130.8, 129.2, 128.7, 128.5, 126.7, 126.5, 126.3, 122.1, 121.9, 117.7, 116.8, 116.65, 116.58, 111.5, 111.2, 110.9, 110.5, 110.1, 110.0, 107.9, 107.6, 80.2, 80.0, 79.8, 56.6, 56.05, 56.00, 55.6, 42.4, 42.1, 41.8, 39.4, 38.7, 37.5, 36.5, 36.4, 28.54, 28.51, 28.4, 28.2, 23.50, 23.47; $[\alpha]_D^{25} +80.6^{\circ}$, (c = 1.0, $CHCl_3$); HRMS: Calcd. for $C_{46}H_{56}N_2O_{11}$ $[M+Na]^+$ = 835.3776 m/z, found = 835.3753 m/z.

(S,S)-tetramethylmagnolamine (1)



20

Chemical Formula: C₄₆H₅₆N₂O₁₁
Molecular Weight: 812.9570



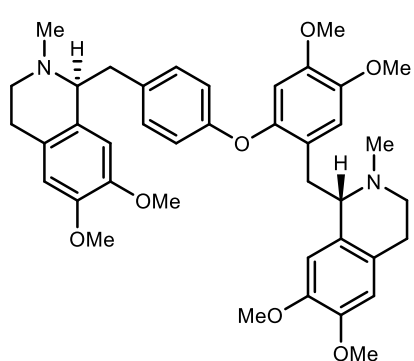
(S,S)-tetramethylmagnolamine (1)
Chemical Formula: C₄₀H₄₈N₂O₇
Molecular Weight: 668.8310

Procedure: A 10 mL flame-dried round-bottom flask equipped with a Teflon-coated stir bar and a rubber septa was charged with **20** (406.5 mg, 0.5 mmol, 1.0 equiv) and Cs₂CO₃ (488.7 mg, 1.5 mmol, 3.0 equiv). The mixture was evacuated and backfilled with N₂ (3 x), prior to the addition of dry and degassed DMSO (2.5 mL). MeI (93.4 μL, 1.5 mmol, 3.0 equiv) was added via micro-syringe, and the mixture was stirred at rt for 12h. The mixture was then poured onto water (20 mL), and washed with EtOAc (3 × 20 mL). The combined organic layers were then washed with water (50 mL), brine (25 mL) and dried over MgSO₄. They were then filtered and concentrated *in vacuo*. The crude reaction mixture was then dissolved in THF (5 mL). LiAlH₄ (189.8 mg, 5.0 mmol, 10.0 equiv) was added, and the reaction mixture was warmed to reflux for 12h. It was then cooled to 0 °C, before the sequential and dropwise addition of water (0.2 mL), 15% aqueous NaOH (0.2 mL) and water (0.4 mL). The resulting biphasic mixture was then stirred for another 30 min. Solid Na₂SO₄ (1 g) was then added to the mixture, and it was then filtered through celite, washed with THF (3 × 20 mL) and concentrated *in vacuo*. The crude product was purified by column chromatography on silica gel (EtOAc:MeOH:NEt₃ 20:1:1), and afforded **1** (145.4 mg, 0.22 mmol, 44%) as a white solid.

Characterization:

R_f = (EtOAc:MeOH:NEt₃ 20:1:1): 0.38; IR (neat) ν = 2993, 2836, 1514, 1500, 1465, 1444, 1254, 1217, 1158, 1138, 1122 cm⁻¹; ¹H NMR (500 MHz, CDCl₃) δ 7.01 (d, J = 8.5 Hz, 2H), 6.76 (d, J = 8.5 Hz, 2H), 6.58 (s, 1H), 6.54 (s, 2H), 6.51 (s, 1H), 6.13 (s, 2H), 3.83 (s, 3H), 3.82 (s, 3H), 3.761 (s, 3H), 3.757 (s, 3H), 3.74 – 3.67 (m, 2H), 3.61 (s, 3H), 3.59 (s, 3H), 3.20 – 3.08 (m, 3H), 3.01 (dd, J = 13.7, 5.9 Hz, 1H), 2.85 – 2.67 (m, 6H), 2.60 – 2.53 (m, 2H), 2.51 (s, 3H), 2.42 (s, 3H); ¹³C NMR (126 MHz, CDCl₃) δ 157.1, 148.1, 147.31, 147.28, 147.1, 146.5, 146.4, 145.3, 133.5, 130.9, 129.8, 129.3, 126.2, 123.8, 115.9, 114.7, 111.25, 111.22, 111.1, 111.0, 105.0, 64.8, 63.3, 56.2, 56.1, 55.84, 55.80, 55.6, 47.0, 46.8, 42.8, 42.7, 40.6, 34.9, 25.8, 25.4; [α]_D²⁵ +81.6°, (c = 1.0, CHCl₃), [lit.⁴ +85.6°, (c = 1.0, CHCl₃)]; HRMS: Calcd. for C₄₀H₄₈N₂O₇ [M+H]⁺ = 669.3534 m/z, found = 669.3522 m/z.

3. NMR Comparison of (S,S)-Tetramethylmagnolamine

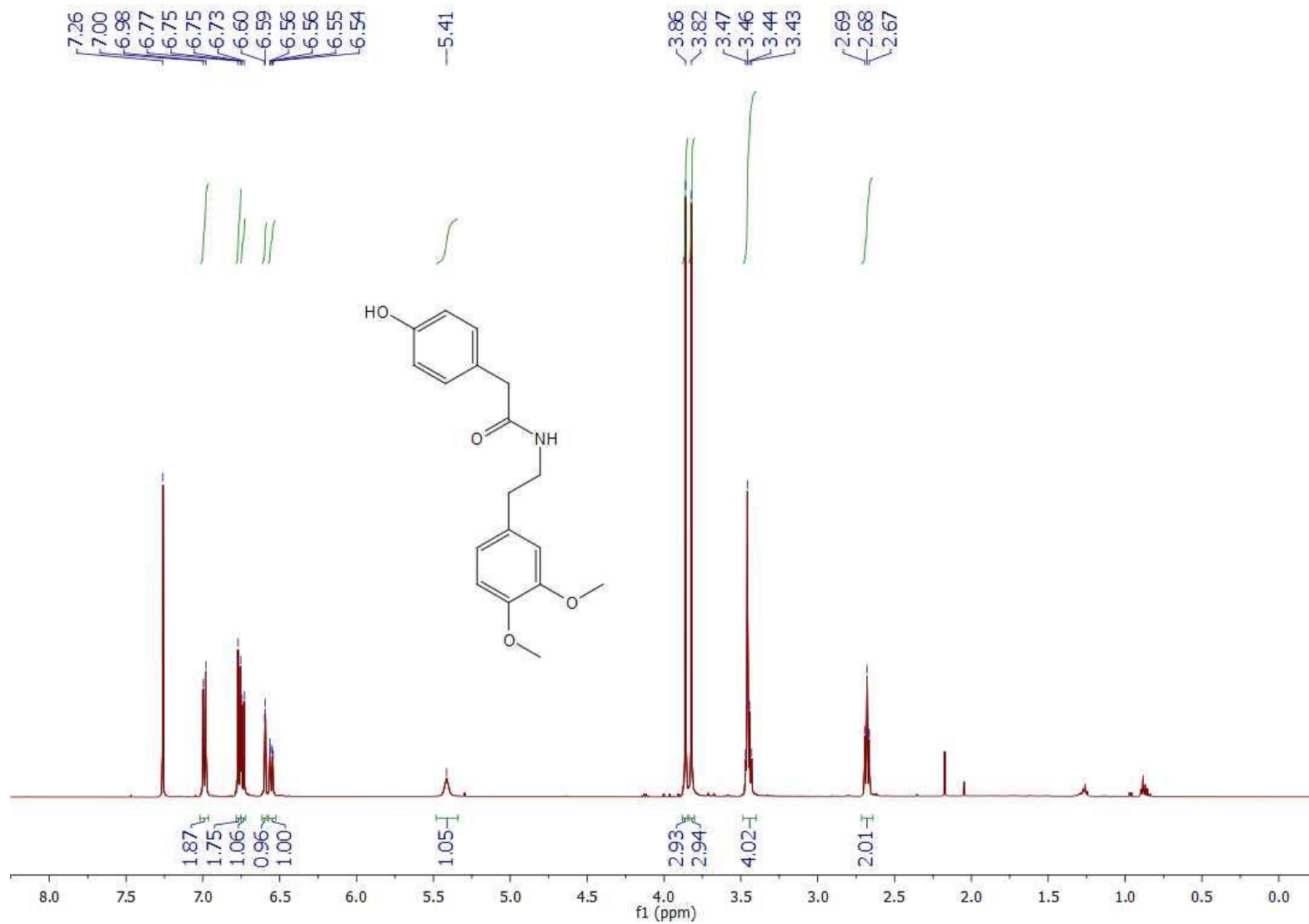
	¹ H-NMR		¹³ C-NMR	
	Literature ⁴	Synthetic	Literature ⁴	Synthetic
Aromatic	7.01 (d, <i>J</i> = 8.8 Hz, 2H)	7.01 (d, <i>J</i> = 8.5 Hz, 2H)	157.2	157.1
	6.76 (d, <i>J</i> = 8.8 Hz, 2H)	6.76 (d, <i>J</i> = 8.5 Hz, 2H)	148.2	148.1
	6.58 (s, 1H)	6.58 (s, 1H)	147.4	147.31
	6.54 (s, 2H)	6.54 (s, 2H)	147.4	147.28
	6.51 (s, 1H)	6.51 (s, 1H)	147.2	147.1
	6.13, 6.12 (2 s, 2H)	6.13 (s, 2H)	146.6	146.5
O-Me	3.83 (s, 3H)	3.83 (s, 3H)	146.5	146.4
	3.82 (s, 3H)	3.82 (s, 3H)	141.5	145.3
	3.76 (s, 3H)	3.761 (s, 3H)	133.6	133.5
	3.76 (s, 3H)	3.757 (s, 3H)	131.0	130.9
	3.61 (s, 3H)	3.61 (s, 3H)	129.8	129.8
	3.58 (s, 3H)	3.59 (s, 3H)	129.3	129.3
N-Me	--	2.51 (s, 3H)	126.3 & 126.3	126.2
	--	2.42 (s, 3H)	123.9	123.8
Aliphatic	3.72 – 3.72, 3.69 – 3.67 (2 m, 2H)	3.74 – 3.67 (m, 2H)	116.0	115.9
	3.20–3.09 (m, 3H)	3.20 – 3.08 (m, 3H)	114.8	114.7
	3.00 (dd, <i>J</i> = 13.4, 6.0 Hz, 1H)	3.01 (dd, <i>J</i> = 13.7, 5.9 Hz, 1H)	111.3	111.25
	2.85 – 2.67 (m, 6H)	2.85 – 2.67 (m, 6H)	111.2	111.22
	2.60 – 2.53 (m, 2H)	2.60 – 2.53 (m, 2H)	111.1	111.1
<div style="text-align: center;">  <p>(S,S)-tetramethylmagnolamine</p> </div>	111.0	111.0		
	106.1	105.0		
	64.9	64.8		
	63.4	63.3		
	56.3	56.2		
	56.2	56.1		
	55.9	55.84		
	55.8	55.80		
	55.7 & 55.7	55.6		
	47.0	47.0		
	46.9	46.8		
	42.9	42.8		
	42.8	42.7		
	40.7	40.6		
	35.0	34.9		
28.8	25.8			
25.4	25.4			

4. References and Notes

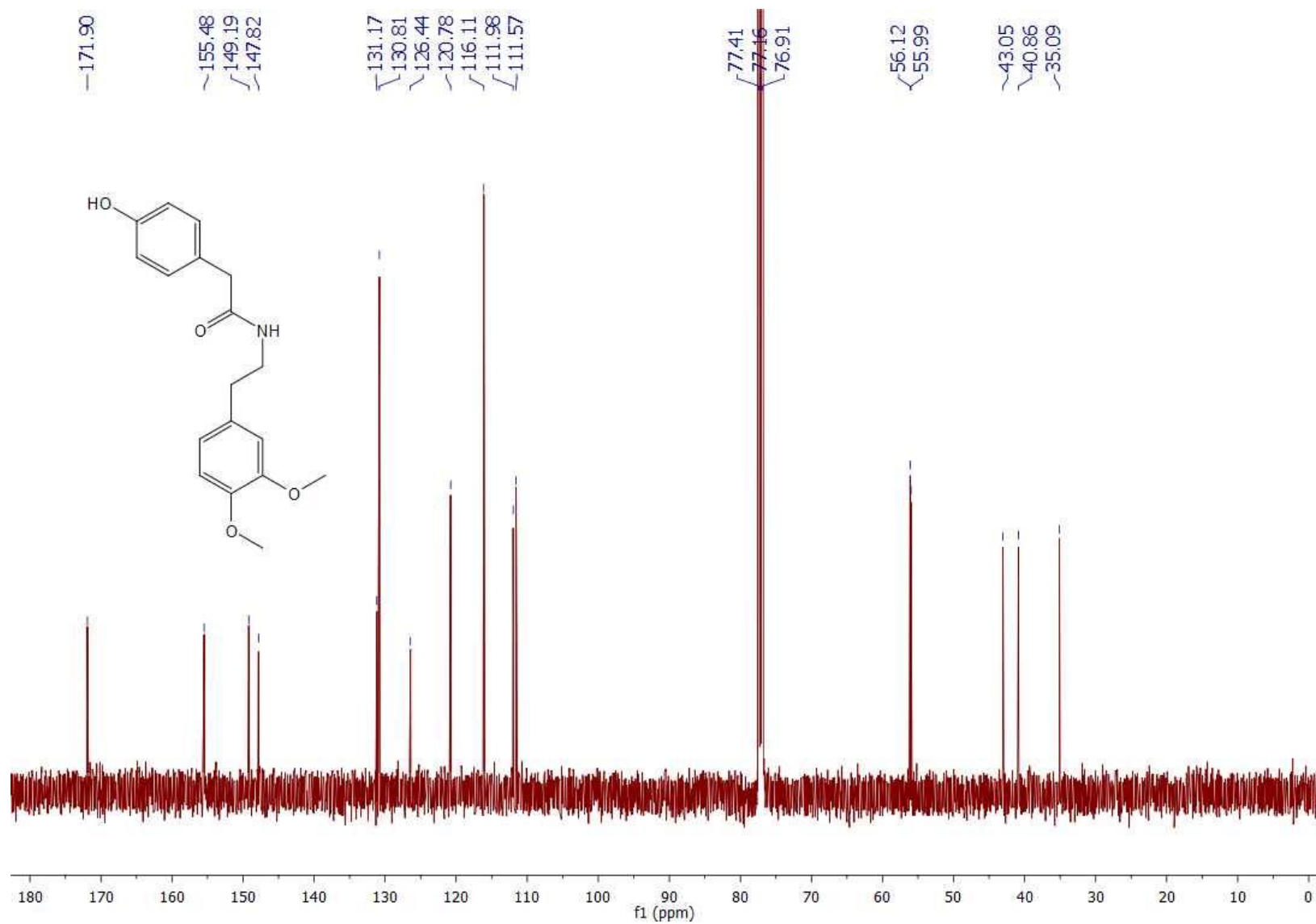
1. L'Homme, C.; Menard, M.-A.; Canesi, S. *J. Org. Chem.* **2014**, *79*, 8481-8485.
2. Kashigaki, K.; Kan, K.; Qais, N.; Takeuchi, Y.; Yamato, M. *Chem. Pharm. Bull.* **1991**, *39*, 1126-1131.
3. Xu, Z.-C.; Wang, X.-B.; Yu, W.-Y.; Xie, S.-S.; Li, S.-Y.; Kong, L.-Y. *Bioorg. Med. Chem. Lett.* **2014**, *24*, 2368-2373.
4. Blank, N.; Opatz, T. *J. Org. Chem.* **2011**, *76*, 9777-9784.

5. Copies of ^1H - and ^{13}C -NMR spectra

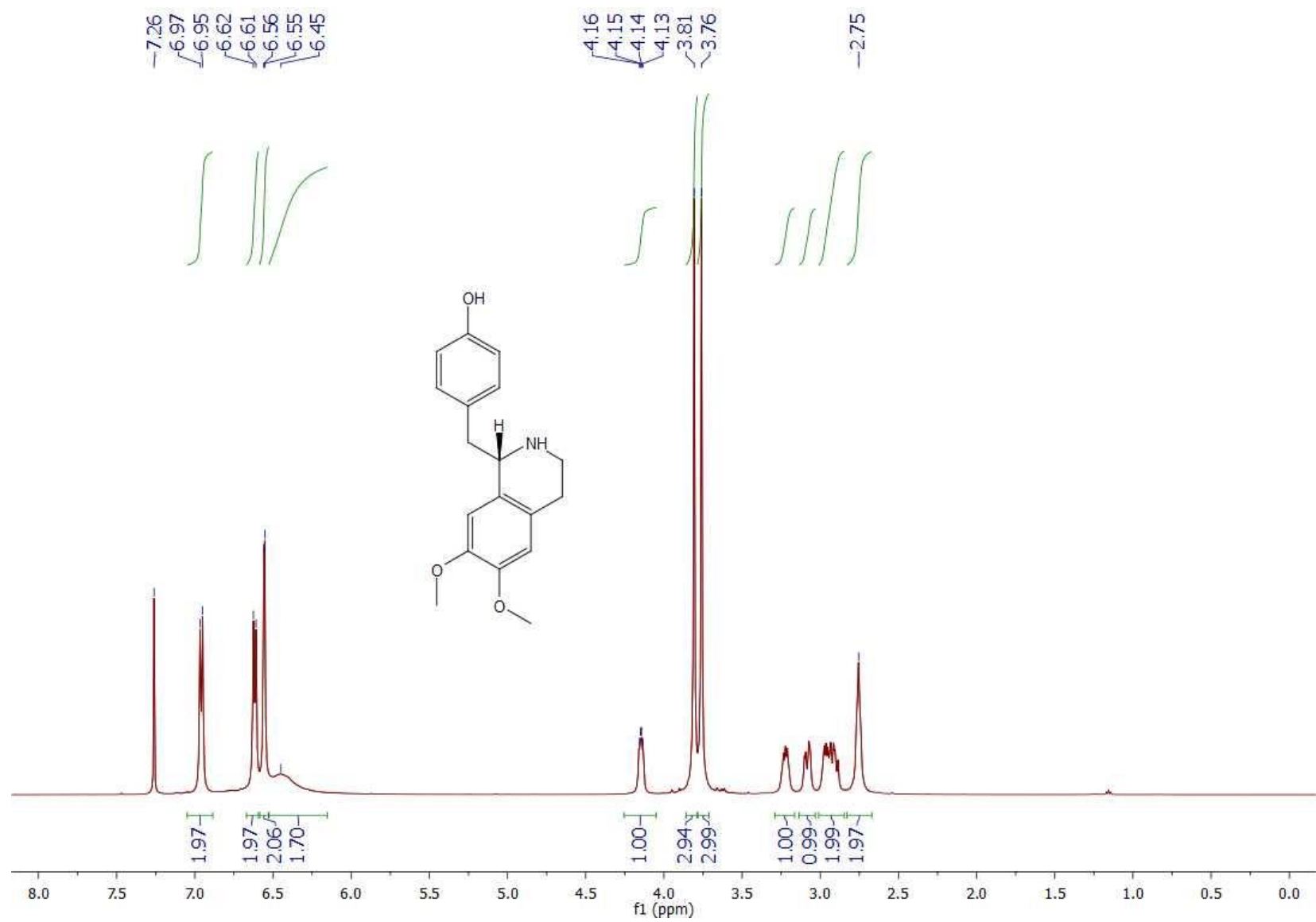
^1H -NMR of compound 14



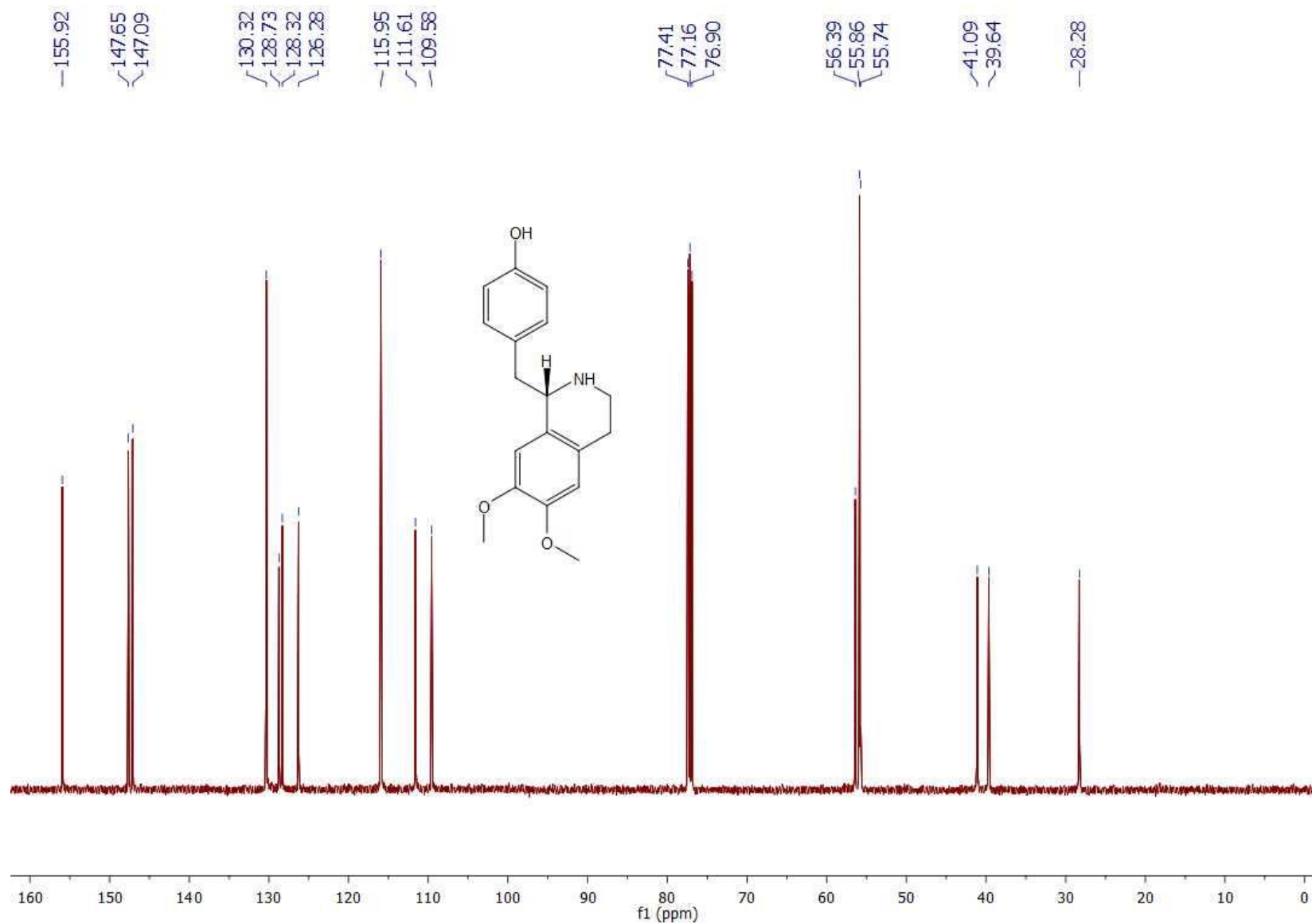
¹³C-NMR of compound 14



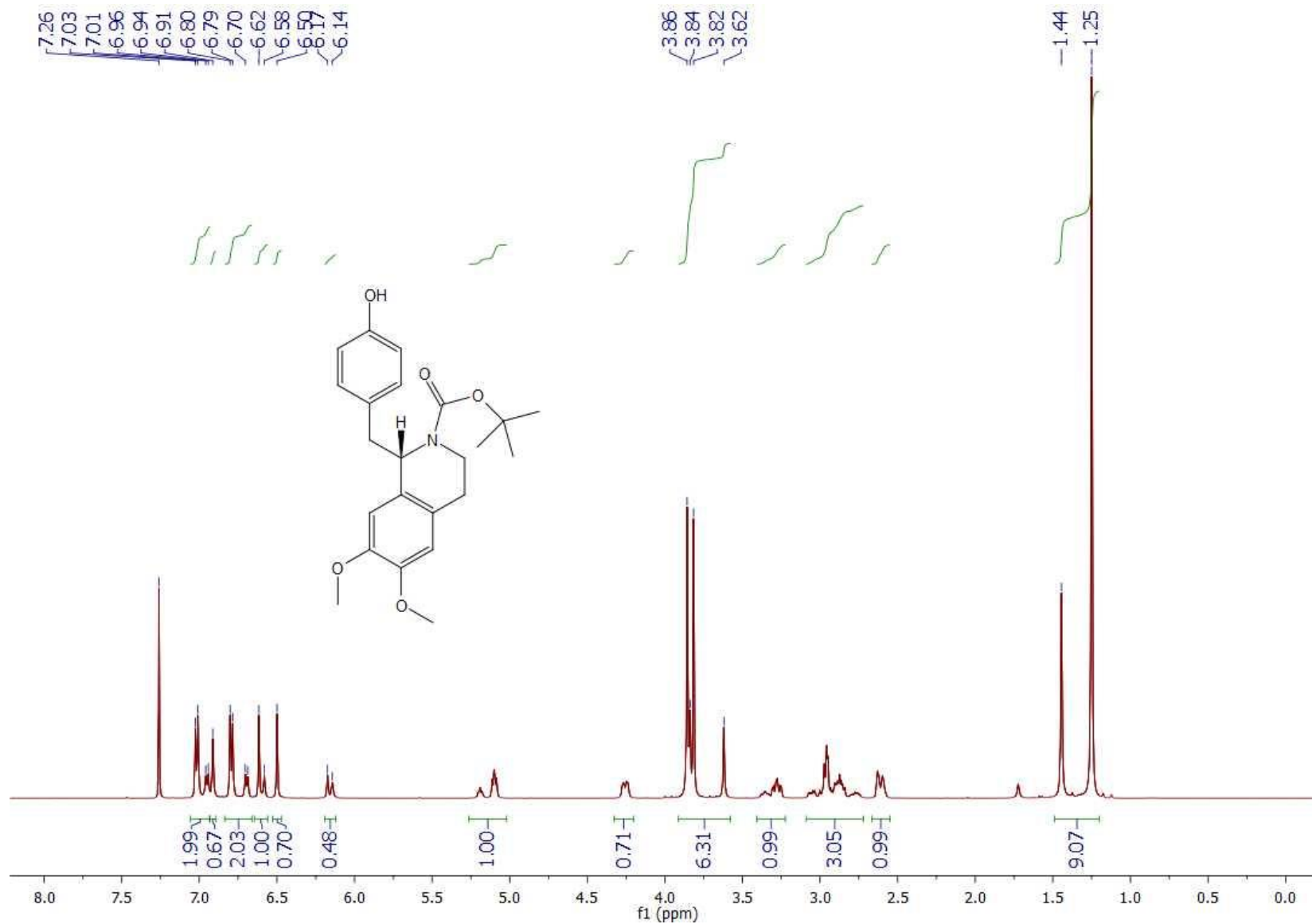
¹H-NMR of compound 16



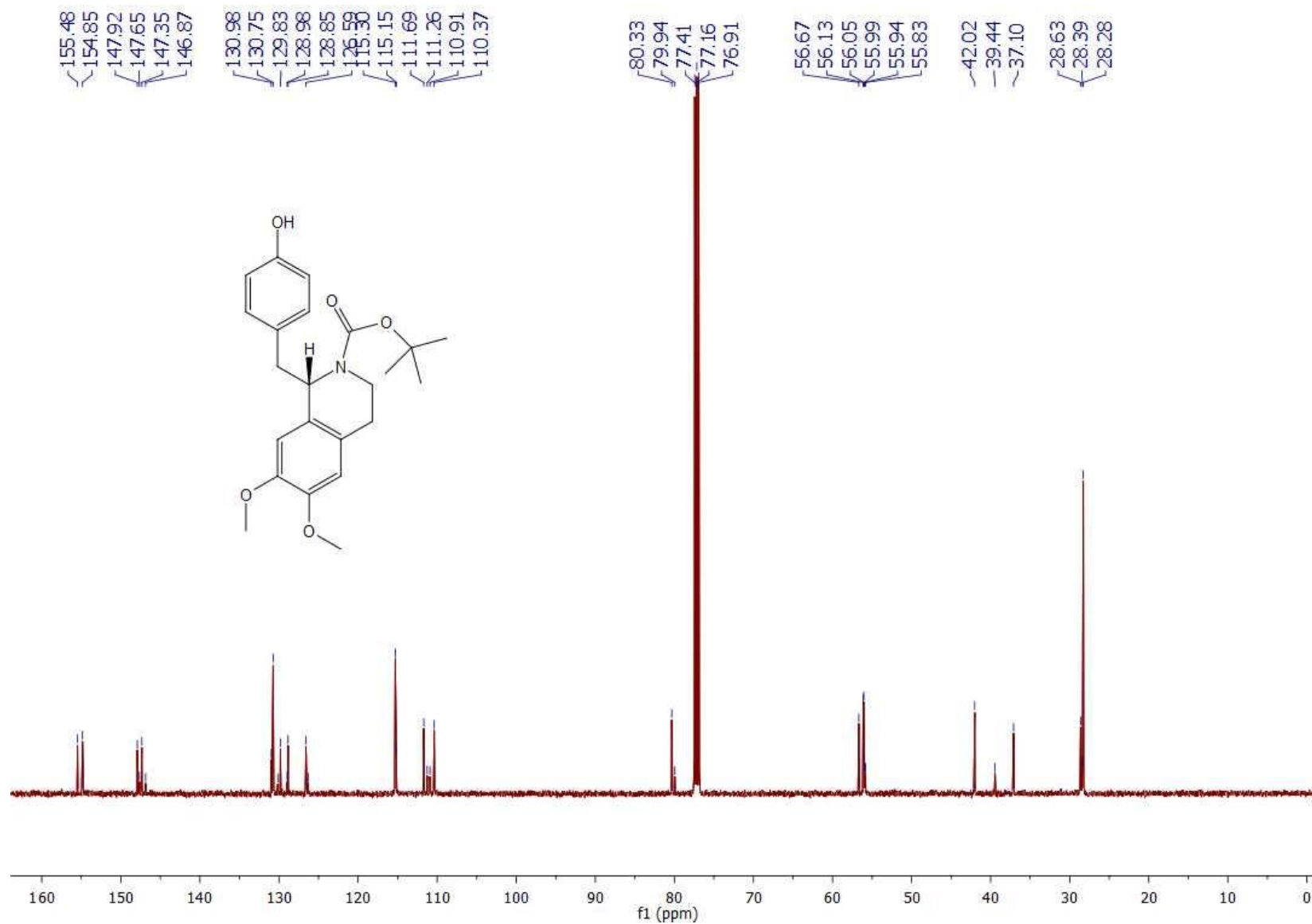
¹³C-NMR of compound 16



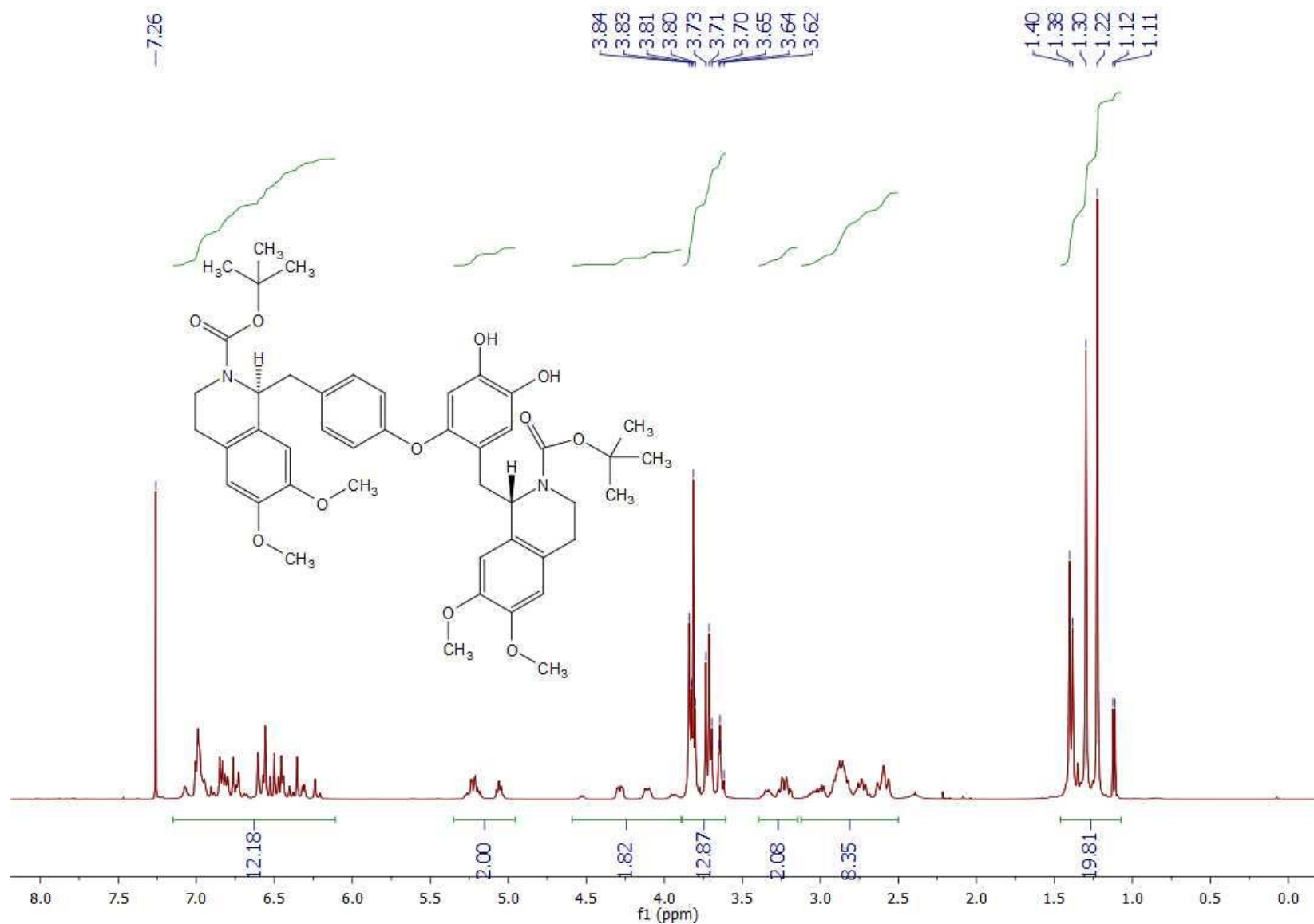
¹H-NMR of compound 17



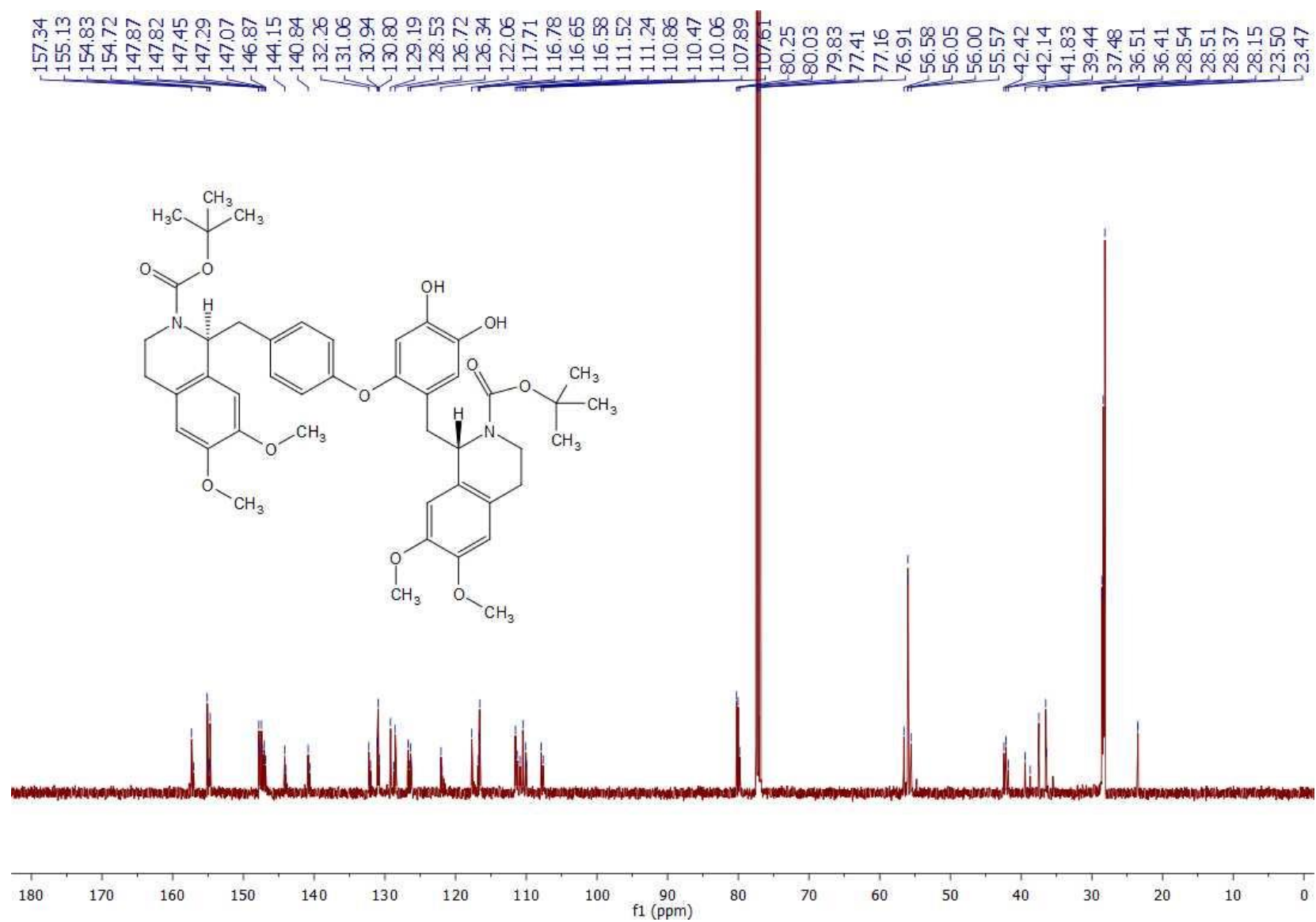
¹³C-NMR of compound 17



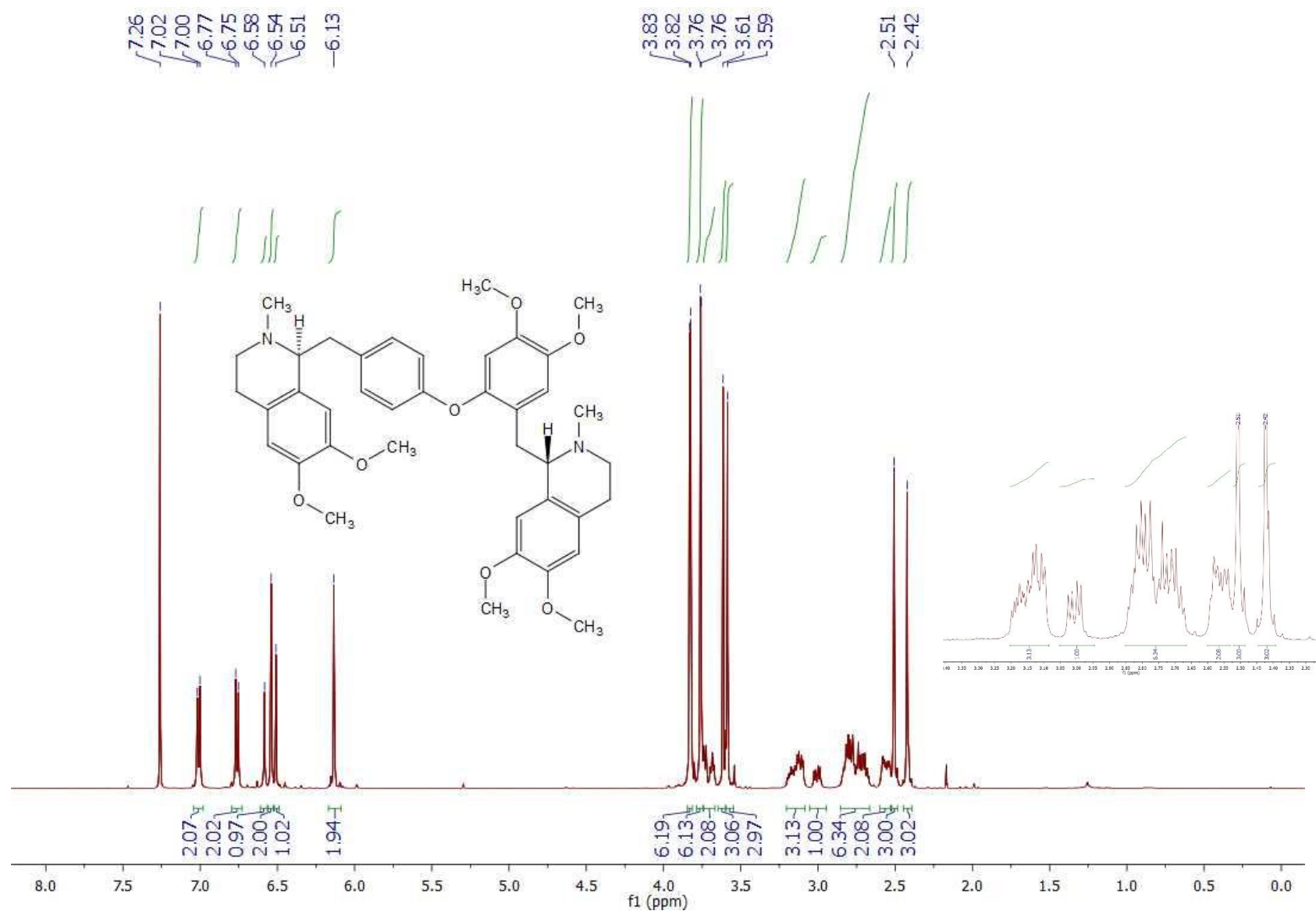
¹H-NMR of compound 20



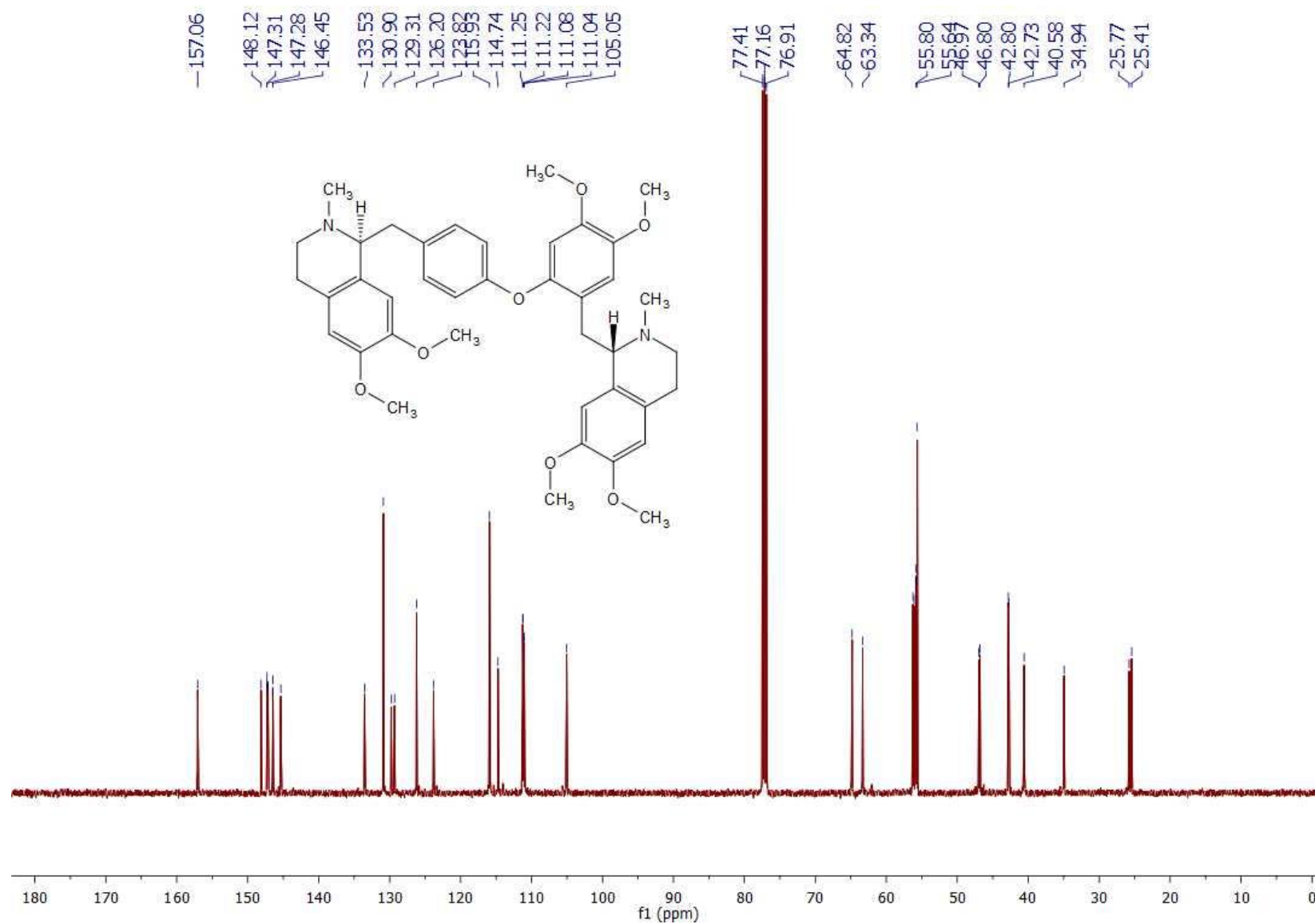
¹³C-NMR of compound 20



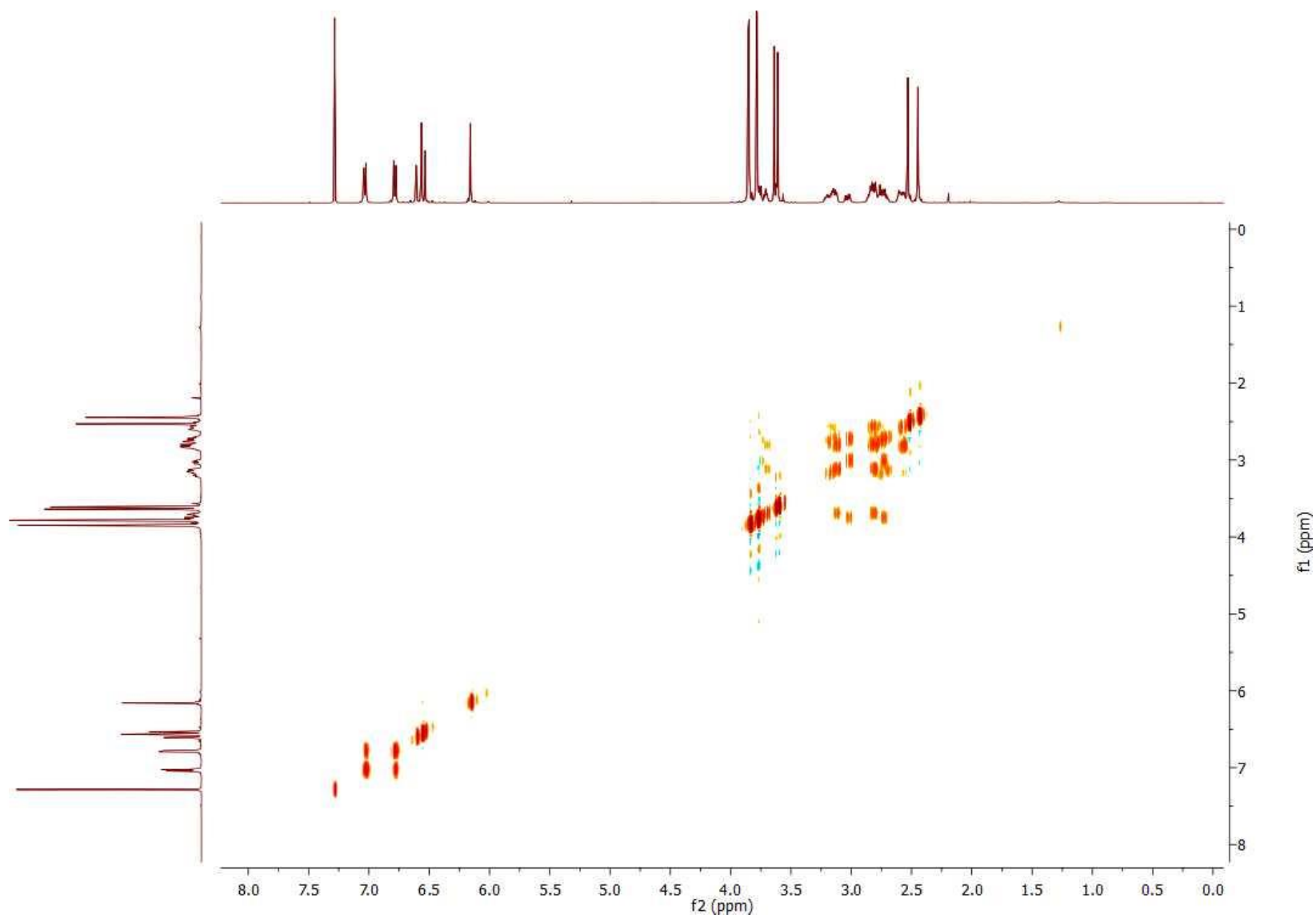
¹H-NMR of (S,S)-tetramethylmagnolamine (1)



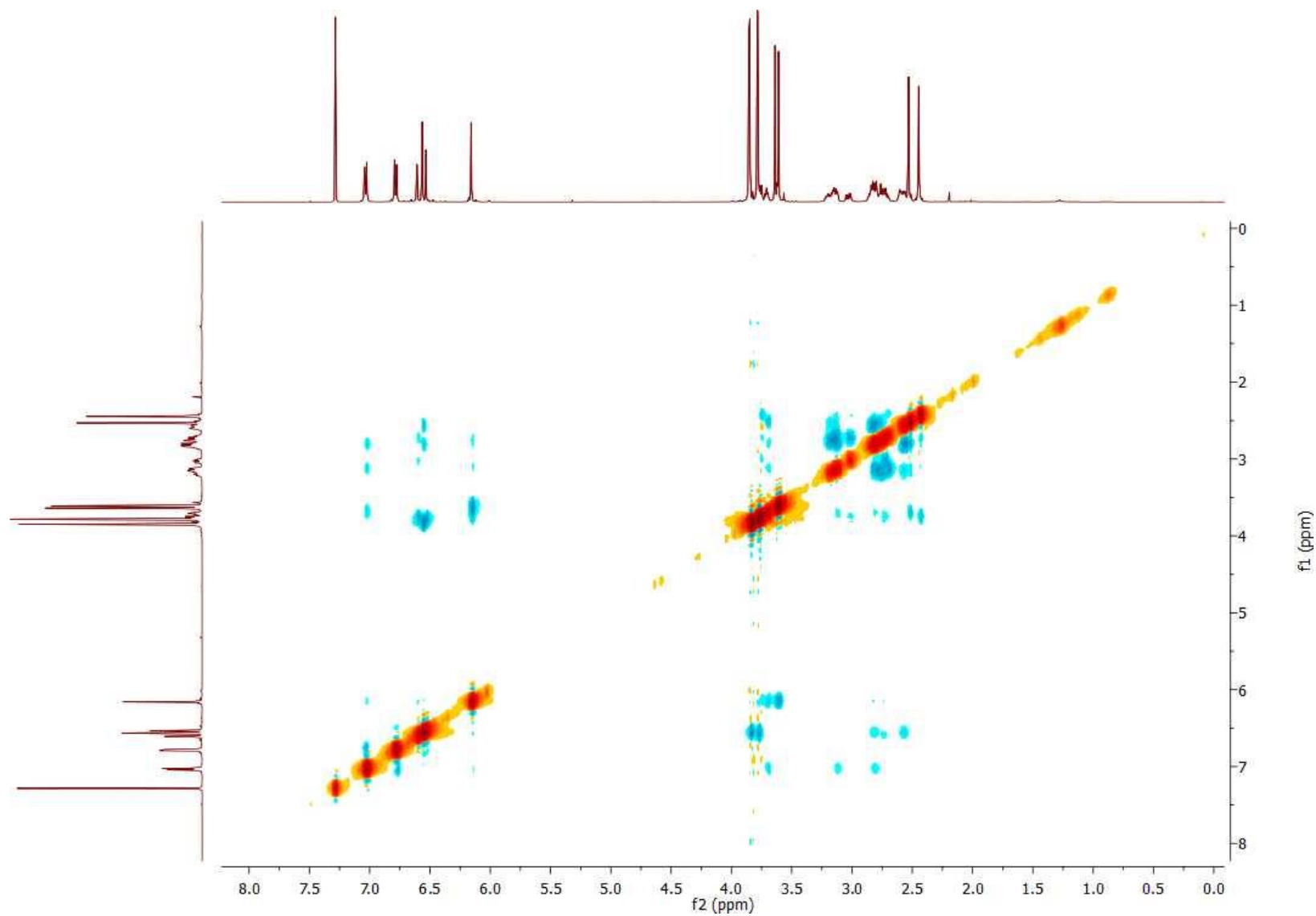
¹³C-NMR of (*S,S*)-tetramethylmagnolamine (1)



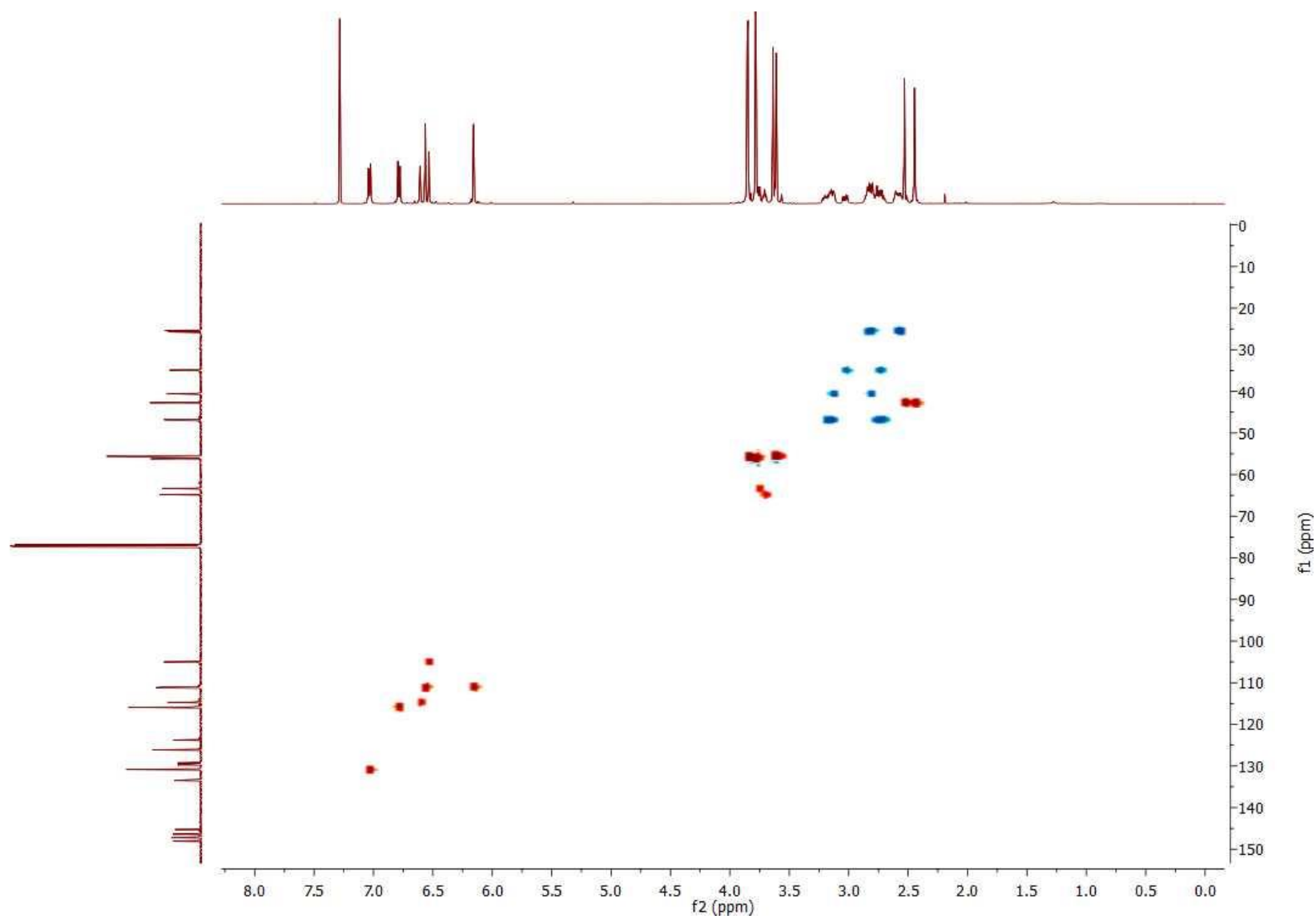
^1H , ^1H -COSY of (*S,S*)-tetramethylmagnolamine (1)



¹H, ¹H-NOESY of (S,S)-tetramethylmagnolamine (1)



^1H , ^{13}C -HSQC of (*S,S*)-tetramethylmagnolamine (1)



^1H , ^{13}C -HMBC of (*S,S*)-tetramethylmagnolamine (1)

